



Assessing the impact of multi-directional ground motion on RC frame buildings: a data-driven approach using vulnerability functions and regression analysis

Moustafa Moufid Kassem¹ · Fadzli Mohamed Nazri² · Zaid A. Al-Sadoon³ · Salmia Beddu¹

Received: 3 July 2024 / Accepted: 1 September 2024
© The Author(s), under exclusive licence to Springer Nature B.V. 2024

Abstract

This research explores the impact of earthquake directionality and orientation on the seismic performance of reinforced concrete (RC) frame structures, an area previously overlooked in seismic design. The multi-directional component of ground motion was not taken into consideration during the seismic performance design of the majority of RC frame structures. Focusing on a case study in Padang City, Indonesia, a region known for moderate seismic activity, this study assesses the behavior of an eight-story ordinary moment resisting frame (OMRF) under various directional components and orientation angles of ground motions. Through Nonlinear Dynamic Analysis (NL-DA) using Nonlinear Time History Analyses (NL-THA), the study incorporates 14 ground motions across East–West and North–South directions, varying from 0° to 60° in 15-degree increments. Incremental Dynamic Analysis (IDA) evaluates the building's response, employing capacity curves, fragility curves, and CMR scores to understand damage probabilities and structural behaviors under different earthquake directions. The objectives include (1) assessing the building's seismic resilience through IDA capacity curves in line with FEMA 356 performance-based design standards, (2) developing fragility curves and the CMR to predict the potential of damages and structural response in various ground motion directions, and (3) formulating a generic relationship between intensity measure (IM), structural behavior (S_B), and incidence angle (θ) via regression analysis. Results highlight the crucial role of θ in influencing structural response, with deterioration in structural behavior noted as the angle of incidence increases. This pattern underscores the varying stress distributions and deformation patterns in response to directional ground movements. The study's findings emphasize incorporating directionality in seismic risk assessments and structural designs, offering valuable insights for improving resilience against future seismic events. Eventually, the link between θ , IM, and S_B is crucial for assessing and mitigating seismic risk, since it indicates that θ is a major element impacting how buildings respond to seismic occurrences.

Keywords Incidence angle · Structural behavior · Intensity measure · Energy dissipation · Fragility curve · CMR · Ground motion · SDG 11

Extended author information available on the last page of the article

1 Introduction

The great majority of engineering stocks are comprised of buildings. However, the most recent dramatic and destructive events (February 2023 in Turkey and Syria, June 2022 in Afghanistan, August 2021 in Haiti, September 2018 in Indonesia, April 2015 in Nepal, and Mac 2011 in Japan and other countries) demonstrated that there was not enough attention paid to the design and construction phases of buildings. This is despite the fact that it is known that in the event of destruction, significant life and financial losses will occur (Essar et al. 2024; Akhoondzadeh 2024; Ghamry et al. 2023; Ramos-Sepúlveda and Cabas 2021). For instance, following the earthquakes that occurred in Turkey and Syria in 2023, the site investigations revealed that almost all the non-engineered reinforced concrete structures had either entirely fallen or suffered from significant damage. The majority of these were not developed and built in conformity with the design codes that were relevant to the situation. (Guo et al. 2024, Ibrahim et al. 2024).

Seismic loadings distinguish themselves from other loads due to the significant deformations and stresses experienced during an earthquake. Seismic performance is determined by specifying the highest acceptable level of damage for a given earthquake ground motion. Codes mandate that structures must have sufficient ductility to enable them to absorb the majority of energy from ground movements through plastic deformations. This idea ensures the structural integrity of structures even in the event of significant damage, as it is typically not cost-effective to design most buildings to withstand moderate-to-strong earthquakes with elastic response. Whereas the seismic performance of reinforced concrete (RC) frame buildings was developed without considering the multi-directional characteristics of earthquake vibrations. Typically, most buildings have been designed by only considering onE-Way analysis for each primary axis separately. However, the dynamic behavior of building structures is influenced by the interaction of several components of an earthquake when considering the probability of seismic occurrences. RC frame buildings are particularly susceptible to damage caused by seismic activity, particularly when exposed to many earthquake orientations.

The influence of earthquakes on engineering construction has been the subject of study for a long time. Many studies show that the effect of earthquakes has changed with respect to incidence angle. Currently, buildings are designed to resist seismic forces by analyzing ground acceleration components and converting them into forces acting in two directions. The issue is in accurately estimating the proportions for applying accelerations and designing seismic forces, since different combinations might result in either excessively cautious or insufficient outcomes. The angle of incidence is crucial in seismic analysis for evaluating the stresses on a structure (MacRae and Mattheis 2000). Athanatopoulou (2005) found that the calculation of interstory drift caused by bi-directional earthquakes relies on the selected reference axis, particularly crucial in irregular buildings. Rigato and Medina (2007) found differences of up to 80% in the greatest inelastic deformations when using angles of incidence other than the typical 0° and 90°. Underestimation in engineering demand parameters can be decreased by up to 20% via performing nonlinear time-history analysis using a significant quantity of data in normal directions and parallel to the fault, as suggested by Reyes and Kalkan (2012).

Reliability in considering the impact of seismic sequences (multi-direction earthquakes) on building behavior is severely lacking in the majority of current design regulations. A single earthquake direction is the basis of the most popular method for seismic design of buildings. The research's findings are restricted and need to go deeper

into investigating the directionality of earthquakes to determine if other seismic demand characteristics are significantly influenced based on the angle of incidence.

The majority of current studies have utilized random earthquakes, whether single or repeated, to examine the response of structures to several seismic events. These studies typically do not take into account the orientation angle of earthquakes. Due to variations in the primary shock or aftershock's properties, such as magnitude, intensity, frequency content, and duration, as well as differences in ground motion characteristics across various site conditions, the obtained data are deemed unreliable. The influence of earthquake direction on the behavior of structures subjected to various directional components of earthquakes is an area that has not been adequately investigated.

This study aims to overcome the limitations by evaluating the seismic performance of an ordinary moment resisting frame (RC-OMRF) building in Padang City, Indonesia. In Padang City, buildings suffered extensive damage because of strong ground shaking and there were widespread and deadly landslides. Most of the buildings damaged or collapsed in Padang city are Reinforced Concrete (RC) frame structures, with some being unreinforced masonry and a few steel building structures. The majority of small structures were constructed with insufficient building materials and exhibited poor expertise. The construction quality of the more recent and larger engineered structures was usually adequate, however there were a few examples of low quality (Irsyam et al. 2020). The significant damage to these buildings raises questions about the effectiveness of design and construction practices, as well as the building code enforcement. In addition, there is a concern to address the seismic performance of RC frame buildings that were designed according to gravity loads only or designed according to current codes (El-Betar 2018). Hence, the structure design in Indonesia should take into account these earthquake activities. To mitigate earthquakes' impact, it is crucial to assess the seismic hazard and incorporate this data into a seismic code for building design and construction.

Consequently, the assessment of this study is conducted by employing Incremental Dynamic Analysis (IDA) as a capacity curve, fragility curves, collapse margin ratio (CMR) scores suggested by FEMA-P695, and regression analysis methodology. These are crucial factors in seismic inquiry used to assess the possibility of damage under various directional components of an earthquake (East-West and North–South) with an increment angle of 15° . A seismic vulnerability function is used to establish the correlation between the severity of an earthquake and the potential impact it may have on the performance of a specific structural system. This research also aims to highlight and demonstrate the substantial impact of the seismic incidence angle on structures. The existing design rules do not account for this particular factor, leading to a potential underestimation of seismic demand even when using advanced dynamic nonlinear code-compliant models. Comprehensive parametric research is necessary to include the impact of seismic incidence angle into the existing building regulations.

Analyzing the multi-directional effects of earthquakes on structures and critical infrastructure is crucial for several reasons:

- Recognizing how buildings respond to seismic difficulties from different orientations improves seismic risk assessment. The research enables engineers and policymakers to determine hazardous regions and recommend retrofitting or strengthening.
- Scientists can develop earthquake-resistant structures and infrastructure by addressing multi-directional seismic loads in structural design. This reduces earthquake collapse and destruction as well as rendering structures safer.

- Community members may lessen the financial impact of earthquake damage by learning about and preparing for the multi-directional effects of these natural disasters on buildings and essential services. This is in line with SDG 11's goals of creating inclusive, safe, resilient, and sustainable cities, and it helps make urban areas more resilient and sustainable in general.

To sum up, improving resilience, guaranteeing safety, and supporting sustainable development goals relating to resilient infrastructure and sustainable urbanization all need comprehensive analyses of the consequences of earthquakes on vital facilities and buildings in all directions.

2 Overview of multi-directional component of earthquake incident angles

Multiple studies indicate that the impact of earthquakes has undergone alterations in relation to the angle at which earthquakes occur. Seismic activity at a particular location on the ground is recorded or detected in two horizontal directions and one vertical direction. According to certain research, it is possible to treat the vertical component of ground motion as uncorrelated with the horizontal components in terms of direction (Penzien and Watabe 1974). The majority of design standards require the simultaneous insertion of two horizontal components so that each earthquake excitation may be effectively addressed (FEMA 2000; EC 2004; TERDC 2007).

In order to demonstrate that structures are affected by the multidirectional component of earthquakes, this study will also center on the directionality of seismic excitations. Magliulo et al. (2014) state that there is a need to consider the influence of earthquake incidence angle, also known as a multi-directional component, in order to gain a better understanding of the seismic performance of building structures that display a typical dynamic behavior. Seismic performance and capacity studies of the chosen RC frame construction must thus take into account the impact of earthquakes' multi-directional components. Before adopting certain judgments during the structural design process to ensure that buildings can withstand future seismic motion, the outcomes of this research will be valuable for critically assessing the influence of directionality on building structures. Therefore, the main goals of this study are to (1) use IDA capacity curves in compliance with FEMA 356 Performance Limit States to figure out the seismic performance of the selected RC-frame structure, (2) Develop fragility curves as a probability distribution function for the chosen RC-frame building in the interaction to strong ground motion in various directions, and (3) Come up with a general formula for the chosen model by combining intensity measure (IM), structural behavior (S_B), and angle of incidence (Φ).

Upon reviewing much research conducted from the past until the present, several investigations have been conducted on the impact of earthquake angles (in two directions) on engineering structures and constructions (González 1992; Rigato and Medina 2007; Fujita and Takewaki 2010; Kostinakis and Athanatopoulou 2015). The study examines structures that experience ground accelerations caused by earthquakes. These accelerations vary between 0° and 90° , and 0° and 180° , with increments of 5° , 6° , 15° , 20° , and so on (Lagaros 2010; Lucchini et al. 2011; Kostinakis et al. 2013; Kumar and Gajjar 2013; Fontara et al. 2015).

Quadri and Madhuri (2014) conducted a study on the critical angle of seismic incidence in reinforced concrete frames. The investigation involves subjecting a four-story reinforced concrete building to earthquake ground accelerations ranging from 0° to 90° , with an increment of 10° . Kanya and Rao (2015) examine the impact of earthquake incidence angle on the seismic performance of reinforced concrete buildings. This study involves the modeling and investigation of one conventional building and two buildings with irregular floor plans. Each building experiences ground accelerations ranging from 0° to 180° . Magliulo et al. (2014) investigated the impact of earthquake direction on the seismic response of irregular planned reinforced concrete frame buildings. The research includes both nonlinear static and dynamic analysis. The incidence angles range from 0° to 330° , increasing by 30° each time. Tanjung and Alfajri (2019) investigated the evaluation of the seismic capacity of an already existing multi-story reinforced concrete structure. Nevertheless, this study solely considers the input in the horizontal X and Y directions for its pushover analysis. The input ground motion utilized in this research was obtained from the recorded seismic events of the 2009 Padang earthquake. Furthermore, Alam et al. (2022) say it's hard to get a good idea of how a building will react to a multidirectional earthquake because the internal forces aren't always distributed in the same way. The ultimate design orientation is ambiguous as a result of the diverse earthquake responses induced by distinct seismic orientations. Nevertheless, according to the fragility analysis results by Gwalani et al. (2021), the failure probabilities of structures are significantly higher when subjected to multi-directional stimulation compared to unidirectional excitation when comparing the estimated seismic collapse capacity.

Nevertheless, numerous studies have examined and developed structures with asymmetrical plans (Nguyen and Kim, 2013), high-rise steel buildings (Tun and Htun 2014), highway tunnels (Sevim 2013), and bridges (Torbol and Shinozuka 2012; Atak et al. 2014; Newton 2014; Ni et al. 2015) based on various seismic excitation angles.

Nonlinear response analysis has often been employed to investigate the impact of earthquake directionality on structures. Cantagallo et al. (2012) conducted a study on the impact of directionality on seismic response variation. They examined the variation of the angle of incidence from 0° to 180° in increments of 22.5° . The study concluded that the main axes of the analyzed structures underestimated the demand, particularly in plan irregular structures. However, structures with double symmetry did not show significant variations. Furthermore, it was noted that the impact of directionality is diminished in scaled seismic recordings. It is important to mention that this study only took into account four structures, hence the findings are restricted in scope.

Fontara et al. (2015) investigated how one-story asymmetric reinforced concrete buildings were affected by the direction and magnitude of seismic activity. A nonlinear relationship existed between the degree of intrusion and the structure's sensitivity to the angle of incidence; the degree of damage directly correlates to the degree of variability in the outcomes as a consequence of the angle of incidence. Typically, one-to four-story reinforced concrete frame structures have been studied utilizing three-dimensional nonlinear time-history analysis to assess the impact of earthquake angle of incidence, without necessarily applying both records at the same time. With increments of incidence angles that vary between 1° and 22.5° , this is found in various papers (Rigato and Medina 2007; Lagaros 2010; Reyes and Kalkan 2015), among others.

Numerous authors have attempted to formulate formulas that estimate, in general, the least desirable angle of incidence or the response it provides. Reinforced concrete building procedures are one example of this (Wilson and Button 1982). Based on modal response spectrum analysis, this method is useful in design, however it ignores earthquake

components acting on the primary structural axis. According to Smeby and Kiureghian (1985), there were certain limitations to the earlier technique. González (1992) has persisted in researching the issue, going so far as to use linear analysis, yielding relative errors of 30% or more. According to, a formula for calculating the critical incidence angle has been put forth by Wilson and Button (1982). This calculation is based on either modal response spectrum analysis or linear response spectrum analysis, which involves five load scenarios and three response spectra.

Following that, a more extensive explanation of the mentioned cited works is given, enabling a deeper understanding of the many approaches used to tackle the problem.

2.1 Method obtained by Wilson Button

The analysis involves considering two response spectra conducted at angles of 0° and 90°. The forces acquired employing the CQC combination are then evaluated, and the critical angle of incidence is determined using the provided formula (Wilson and Button 1982).

$$\tan(2\theta_{cr}) = 2f_0f_{90} \frac{1 + \alpha^2}{(f_0^2 - f_{90}^2)(1 - \alpha^2)} \tag{1}$$

where α is the factor that multiplies the response spectrum and f_0 and f_{90} are the responses obtained for an angle of incidence of 0 and 90, respectively.

2.2 Method obtained by López and Torres

The authors suggest using modal response spectrum analysis to address directionality in five load cases.

The suggested method is:

- Solving five spectral modal load situations for response parameters.
- Eq. (2) calculates critical incidence angle.
- Eq. (3) yields maximum responses for each critical angle of incidence.

$$\theta_{cr} = \frac{1}{2} \tan^{-1} \left(\frac{2 \sum_i \sum_j C_{ij} [R_i^{2y} R_j^{2x} - R_i^{1x} R_j^{1y}]}{(R^{1y})^2 + (R^{2y})^2 - (R^{1x})^2 + (R^{2x})^2} \right) \tag{2}$$

$$R(\theta) = \{ [(R^{1x})^2 - (R^{2y})^2] \cos^2(\theta) + [(R^{1y})^2 - (R^{2x})^2] \sin^2(\theta) + 2 \sin(\theta) \cos(\theta) \left[\sum_i \sum_j C_{ij} R_i^{1x} R_j^{1y} - \sum_i \sum_j C_{ij} R_i^{2y} R_j^{2x} \right] + (R^3)^2 \}^{1/2} \tag{3}$$

where R is the peak response of the chosen parameter, C is the participation coefficient, and θ_{cr} is the critical incidence angle.

2.3 Method obtained by Dongsheng et al.

This approach is a simplified form of the CQC3 method. The SRSS3 approach, which was initially proposed by Gao et al. (2004), is prone to significant mistakes when there is a strong correlation among the vibration modes of the structures. However, it yields comparable findings to the CQC3 method in cases where such correlation is not present. The formulas provided below consider the proportional correlation throughout the design spectra in each direction of assessment.

$$R^{1x} = \sum_i R_i^{1x} R_i^{1x} \tag{4}$$

$$R^{1y} = \sum_i R_i^{1y} R_i^{1y} \tag{5}$$

$$\theta = \frac{1}{2} \tan^{-1} \left(\frac{2 \sum_i R_i^{1x} R_i^{1y}}{(R^{1x})^2 - (R^{1y})^2} \right) \tag{6}$$

$$R(\theta) = \left[(R^{1x})^2 + (\xi R^{1y})^2 \right] \cos^2(\theta) + \left[(R^{1y})^2 + (\xi R^{1x})^2 \right] \sin^2(\theta) \tag{7}$$

$$+ 2 \sin(\theta) \cos(\theta) (1 - \xi^2) \sum_i R_i^{1x} R_i^{1y} + R^{32})^{1/2}$$

2.4 Method obtained by Menun and Der Kiureghian

The authors suggest employing the CQC3 combination as a substitute for the multicomponent. Utilizing a combination of SRSS, CQC, and either the 30% or 40% guidelines is being suggested as an alternative approach (Menun and Der Kiureghian 1998).

$$R_K^2 = \sum_i \sum_j \rho_{ij} \alpha_{kj} \alpha_{ki} S_{ki} S_{kj} \tag{8}$$

$$R_{kl}^2 = \sum_i \sum_j \rho_{ij} \alpha_{ij} \alpha_{ki} S_{ki} S_{lj} \tag{9}$$

$$\theta_{cr} = \frac{1}{2} \tan^{-1} \left[\frac{\frac{2}{\xi} R_{12}}{R_1^2 - \frac{1}{\xi^2} R_2^2} \right] \tag{10}$$

2.5 Method obtained by Athanapoulou et al.

The researchers introduced an analytical technique to calculate the crucial angle of incidence for structures that experience three associated earthquake components. This necessitates analyzing three time-history situations, one for each component, without utilizing the Penzien and Watanabe model (Penzien and Watabe 1974). Linear behavior is assumed, as response spectra cannot be employed due to the assumption of record correlation.

Figure 1 displays the reference axes that were taken into account, together with a graphical depiction of the suggested reactions.

The following equations are required to calculate the critical angle. θ_{cr1} represents the angle at which the maximum response is achieved, whereas θ_{cr2} represents the angle at which the minimum response of the envelope R_0 is reached, taking into consideration the signs.

$$R_0(t_{cr})^2 = R_x(t_{cr})^2 + R_y(t_{cr})^2 \tag{11}$$

$$\theta_{cr1} = \tan^{-1} \left(\frac{R_y(t_{cr1})}{R_x(t_{cr1})} \right) \tag{12}$$

$$\theta_{cr2} = \tan^{-1} \left(\frac{R_y(t_{cr2})}{R_x(t_{cr2})} \right) - \pi \tag{13}$$

where t_{cr1} and t_{cr2} represent the specific moments in time when the highest positive and lowest negative displacements take place.

2.6 Method obtained by Anastassiadis et al.

This approach relies on response spectra for the presence of a primary axis aligned with the epicenter, a secondary axis perpendicular to it, and a tertiary axis in the vertical direction.

The seismic design proposed relies on identifying the optimal orientation that produces the highest response. It involves calculating the maximum and minimum response

Fig. 1 Displacement representation relative to the reference axis (Athanapoulou et al. 2005)

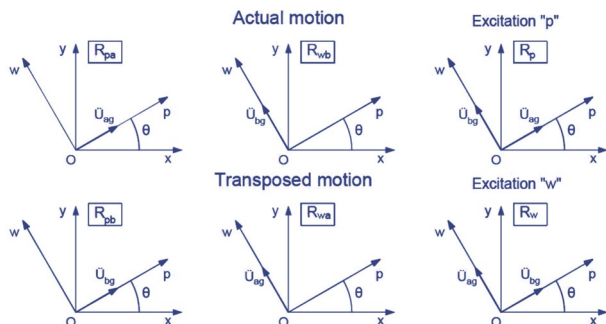
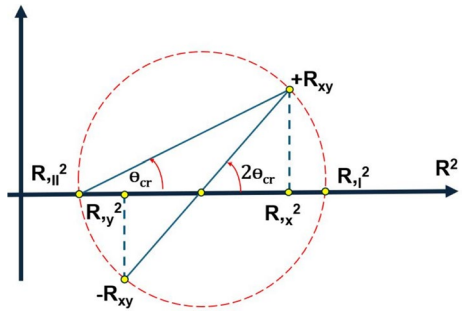


Fig. 2 Utilization of the Mohr circle for graphical representation



parameters and applying the severe stress or force method to identify the most undesirable combination of stresses posing on particular structural components (Anastassiadis et al. 2002). A graphical representation of the response reaction can be calculated using Mohr's circle as shown in Fig. 2.

$$\theta_{cr} = \begin{cases} \frac{1}{2} \tan^{-1} \left(2 \frac{R_{xy}}{R_x^2 - R_y^2} \right) \\ \theta_0 + \frac{\pi}{2} \end{cases} \quad (14)$$

$$\max R^2 = \frac{(R_x^2 + R_y^2)}{2} + \left(\left(\frac{R_x^2 + R_y^2}{2} \right)^2 + R_{xy}^2 \right)^{0.5} \quad (15)$$

$$\min R^2 = \frac{(R_x^2 + R_y^2)}{2} - \left(\left(\frac{R_x^2 + R_y^2}{2} \right)^2 + R_{xy}^2 \right)^{0.5} \quad (16)$$

$$R_x^2 = R_{xa}^2 + R_{yb}^2 = \sum_i \sum_j \varepsilon_{ij} (R_{i,xa} R_{j,xa} + R_{i,yb} R_{j,yb}) \quad (17)$$

$$R_y^2 = R_{xb}^2 + R_{ya}^2 = \sum_i \sum_j \varepsilon_{ij} (R_{i,xb} R_{j,xb} + R_{i,ya} R_{j,ya}) \quad (18)$$

$$R_{xy} = R_{xy,a} - R_{xy,b} = \sum_i \sum_j \varepsilon_{ij} (R_{i,xa} R_{j,ya} - R_{i,xb} R_{j,yb}) \quad (19)$$

Fig. 3 3D view of the selected model

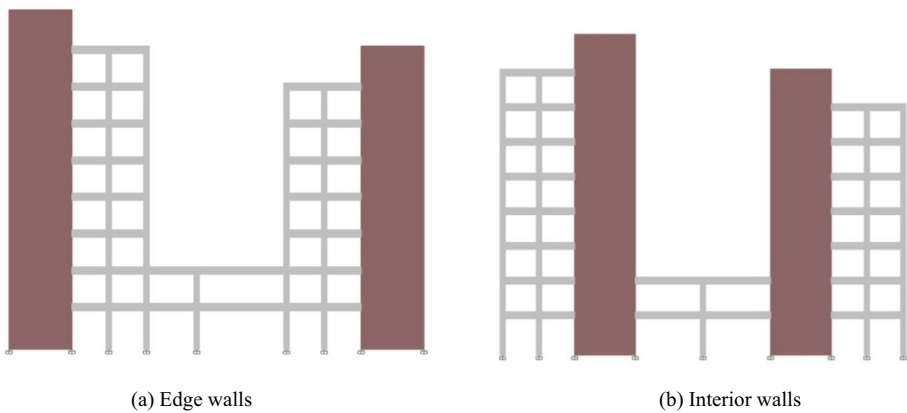
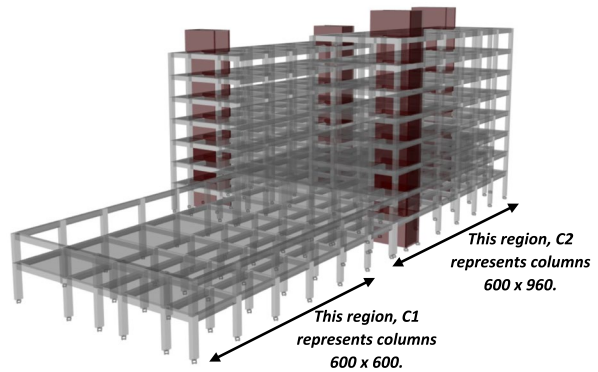


Fig. 4 2D views of the 4-shear walls located at the edge and interior of the selected models

2.7 Method obtained by Lagaros

The researchers of this method have proposed a method called Multidirectional Incremental Dynamic Analysis (MIDA) for performance-based design. This method utilizes pairs of records and incident angles generated by Latin hypercube sampling (LHS) to consider the variability of seismic excitation and the angle of incidence (Lagaros 2010). Two structures, one symmetric and one asymmetric, both consisting of three stories, were evaluated. The analysis took into account fifteen recordings and an incidence angle ranging from 0° to 180° . Afterwards, the MIDA and its corresponding representative MIDA curve were executed.

3 Numerical modelling and description of the selected RC frame building

In this study, an eight-story (G+7) ordinary moment resisting frame (OMRF) structure, in Padang City, Indonesia is selected as a case study to examine the seismic scenario due to multiple components of earthquake directions. The building has eight stories with an inter-story height equal to 4.0 m except ground floor that is 5.0 m height in which can be classified as soft story. The total height of the building is equal to 37.0 m. A 3D-model with detailed structural configurations is shown in Fig. 3. The building consists of 4 shear walls located at the edge and inner side of the building as shown in Fig. 4. It is assumed that the selected building is a step back type of RCMRF system and it is designed as per Eurocode 2 (EC2) and analyzed using Finite Element (FE) platform.

It is important to note that this study focuses solely on the use of reinforced concrete as a building material for multistory structure. It has been assumed that the characteristic strength of concrete in this building configuration is 25 MPa, and that the characteristic strength of the steel reinforcement is 420 MPa. These are the material attributes of

Table 1 Detailing of steel reinforcement in shear walls

Shear wall reinforcement details	Longitudinal reinforcement	Transverse reinforcement
Zone A	10 T 20	T12 @ 200
Zone B	18 T 20	T12 @ 200
Panel 1	–	T12 @ 400
Panel 2	28 T 16	T12 @ 400
Panel 3	28 T 16	T12 @ 400

Table 2 Detailing of steel reinforcement in columns

Column reinforcement details	Column size	Longitudinal reinforcement	Transverse reinforcement
C1	600×600	20 T 16	T10 @ 250
C2	600×960	20 T 16	T10 @ 250

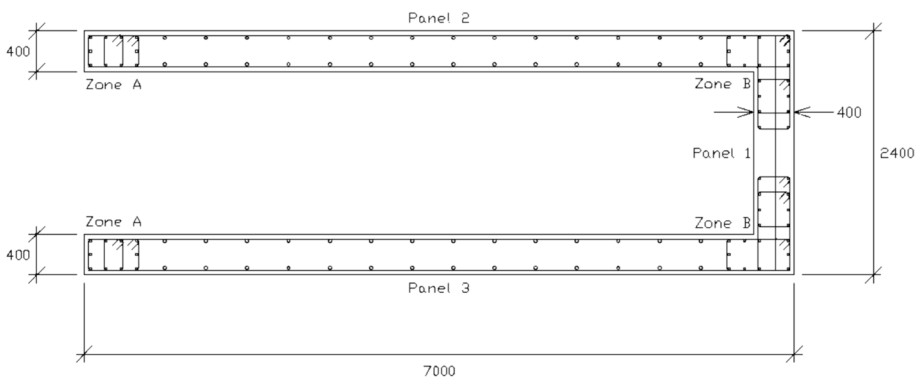


Fig. 5 Steel reinforcement detailing in shear walls (dimensions are in mm)

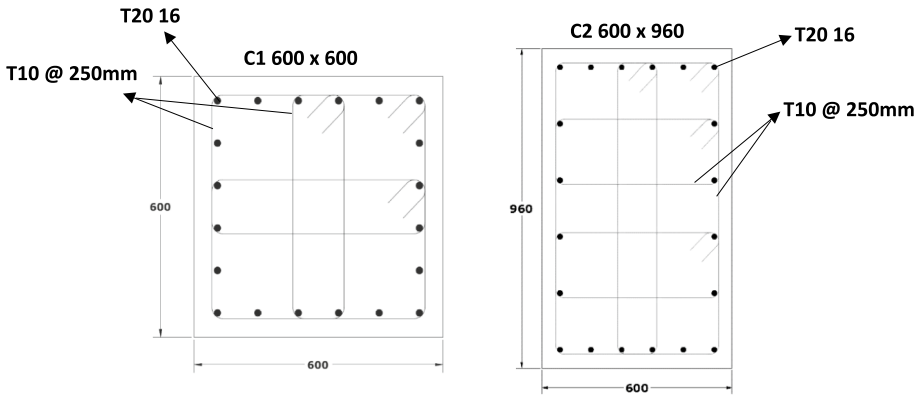


Fig. 6 Steel reinforcement detailings in columns (dimensions are in mm)

the building configuration. The three-dimensional model of the building was created by employing Finite Element software designed specifically for structural research. Slabs of 200mm thickness have been classified as rigid diaphragms, whereas structural elements such as beams, and columns have been modeled using 3D frame elements. The building's live and dead loads have been determined in accordance with Eurocode 2 (EC2), where the load pattern of the dead load (G_k) equals to 1.5kPa, and live load (Q_k) equals to 2.5kPa. Each of the featured structures was thoughtfully designed to withstand a variety of different types of gravity-based design loads, all in accordance with the requirements of European regulations (EC2). The reinforcement detailing for the shear walls and the columns are shown in Tables 1 and 2, respectively. Figures 5 and 6 show the geometric section and its detailing for shear walls and columns, respectively.

4 Overview of research methodology application

In this study, the overall workflow of the research, beginning with the desk study and progressing to the seismic analysis, is depicted in Fig. 7. Using the FE software, a Non-linear Dynamic Analysis (NL-DA) is being performed on a 3D model that is being represented by an RC Frame building. This analysis is followed by a Nonlinear Time History Analysis (NL-THA), which is defined by selecting a set of ground motion records and considering earthquakes with multi-directional components in the X and Y directions. There are five earthquake angles that are specified respectively in both the X-Longitudinal Direction (E–W) and the Y-Transverse Direction (N–S), ranging from 0° to 60° angle with an angle increment of 15° . These angles are specified in both the X-Longitudinal Direction and the Y-Transverse Direction as schematized in Fig. 8a, b that further response quantifications parameters using Intensity Measure (IM) and Damage Measure (DM) are needed for seismic risk analysis.

Despite this, the seismic risk evaluation of the chosen structures is performed by creating dynamic capacity curves, also known as incremental dynamic analysis (IDA) curves, for each directional component (ranging from 0° to 60°). The IDA curves can be

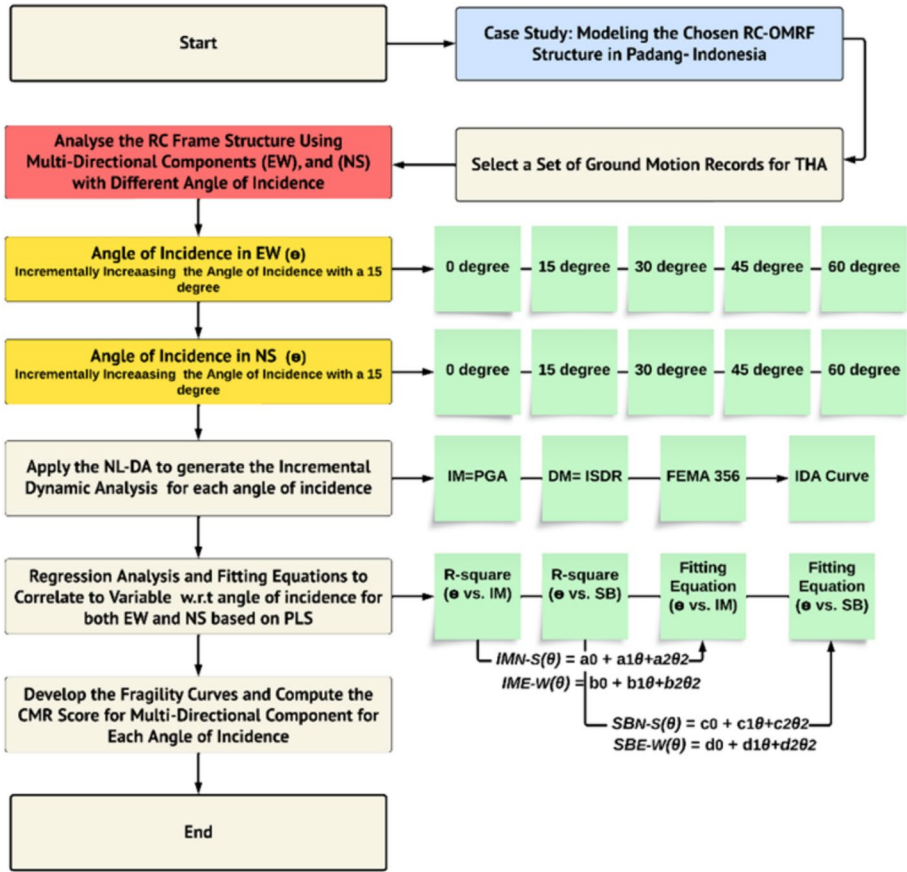


Fig. 7 The overall framework uses a multidirectional earthquake component that contributes to the analysis of the influence of seismic behavior on RC frame building

generated by utilizing the relationship between the inter-story drift ratio, also known as the (ISDR), and the intensity measure (IM) of the ground motion, which is represented by Peak Ground Acceleration (PGA). Using the drift ratios specified by FEMA 356, this relationship is employed to evaluate the building’s seismic performance within a pre-determined performance limit condition.

Furthermore, the fragility curves are then generated using a cumulative distribution function (CDF) which is known as probabilistic approach that shows the probability of damage based on three performance limit states or damage states. Fragility curves are utilized in an analytical framework to evaluate the risk of the seismic influence on the structural models. These curves are regarded as valuable tools for predicting the probability of damage to any structural systems. The performance levels that specify the damage states of the selected models are: Immediate Occupancy (IO, ISDR = 0.50%), Life Safety (LS, ISDR = 1.50%) and Collapse Prevention (CP, ISDR = 2.5%).

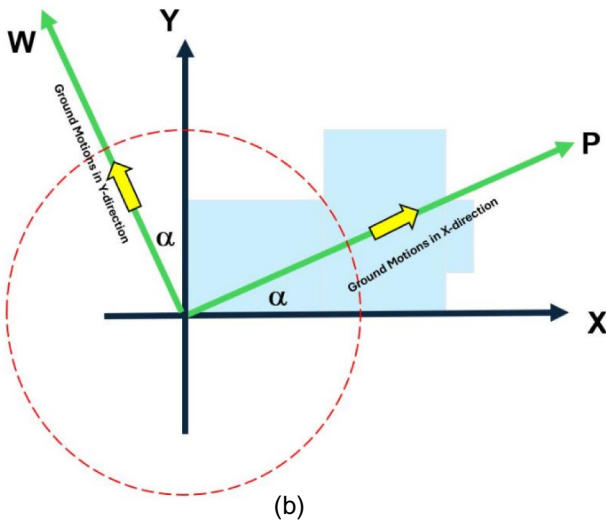
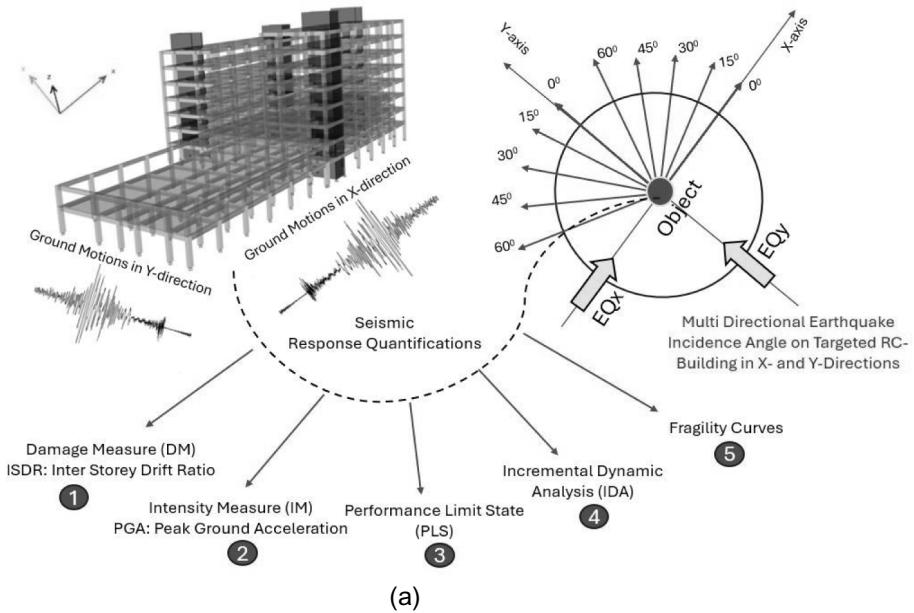
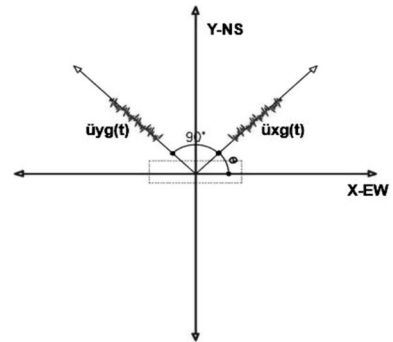


Fig. 8 **a** Quantification of seismic response outcomes; **b** Orientation of earthquake excitation directions relative to the x and y axes characterized by the angle of incidence

5 Criteria to collect set of ground motion records according to their angle of incidence

In order to assess the impact of ground motion rotation, the acceleration components $\ddot{u}_x(t)$ and $\ddot{u}_y(t)$ in the orthogonal (x and y) directions are rotated by the specified angle and then resolved into the degrees of freedom of the structure (Fig. 9). It is commonly

Fig. 9 Rotation of ground motion acceleration



acknowledged that initially, the vectors $\ddot{u}_xg(t)$ and $\ddot{u}_yg(t)$ are oriented along the X and Y directions, respectively.

The nonlinear time history analysis, also known as NL-THA, is the method that provides the highest level of accuracy for evaluating the seismic risk of building structures. It is able to make accurate predictions of the inelastic demands placed on the members of the superstructure in response to a diverse set of earthquake situations. In order to utilize the Non-Linear Time History Analysis, one of the most important steps that must be taken is to identify sufficient ground motion records. This is also one of the most important factors that must be considered in order to ensure a valid simulation process. Three or seven ground motions are required, depending on the ASCE/SEI 7–10 (ASCE 2017), in order to provide an unbiased examination of the structural response of the building.

The building is an office structure categorized as Seismic The spectral parameters SS, which represents the spectral acceleration at short period, and S1, which represents the spectral acceleration at 1 s, are obtained from the Indonesian Spectral Map. These spectra are generated for the Maximum Considered Earthquake (MCE), defined as an earthquake with a 2% probability in 50 years or a seismic event with a return period of 2500 years. In accordance with the desired response spectrum specified in the Indonesian seismic code, this analysis employs seven sets of historically ground accelerations that have been scaled spectrally in order to produce scaled time-history accelerations. Subsequently, these scaled time-history accelerations are applied to the structural model using finite element analysis for nonlinear time-history analysis. The scaled earthquake ground motion recordings are used to dynamically simulate and quantify seismic risk. This is done by generating IDA curves, followed by fragility curves using performance limit states such as IO, LS, and CP.

To explore how the seismic action's angle of incidence affects the structure, it's crucial to specify that the symmetry under investigation pertains to the orientation plane of the structural axes (x and y). This study does not take into account any asymmetry in elevation with respect to the z-axis. In this study the conventional axes depicted in Fig. 9 as our reference, where x and y denote the orthogonal axes defining the structure, commonly used in its design and analysis. Meanwhile, w and p represent the axes on which the pair of records was applied for nonlinear time-history analysis, with w being the longitudinal component and p the transverse component. Each record's pair of components underwent a variation at intervals of 15°, spanning from the 0° position to the 90° position.

All fixed-base models undergo nonlinear time history analysis in accordance with seismic code SNI 1726:2019 (SNI1726:19 2019). According to the code, input ground motions from earthquakes produced by the megathrust, Benioff, shallow crustal, and

Table 3 Database of resilient seismic records for nonlinear structural response analysis

Selected Ground Motion Records for Time History Analysis (THA)							
Mechanism	Data Code	Direction	Magnitude Mw	Epicentral Distance (km)	Station	Event Name	PGA (g) Duration (sec)
Megathrust	MYG013EW	EW [0°-60°]	9.0	170	K-NET, Miyagi	Tohoku Earthquake,	0.792 262.49
	MYG013NS	NS [0°-60°]					
Megathrust	212V5090	EW [0°-60°]	7.7	42.8	PEER, Sitka Observatory	Sitka Earthquake	0.248 55.1
	212V5180	NS [0°-60°]					0.235
Benioff	TCU089-W			7.0	PEER, Taiwan Central Weather Bureau	Chi-Chi Earthquake	0.271 79.0
	TCU089-N						0.344
	TCU120-N	EW [0°-60°]	7.6	25.6	PEER, Taiwan Central Weather Bureau	Chi-Chi Earthquake	0.259 90
	TCU120-W	NS [0°-60°]					0.261
Shallow Crustal	TCU136-E				PEER, Taiwan Central Weather Bureau		0.281
	TCU136-N						0.259
Shallow Crustal	MEL090	EW [0°-60°]	7.3	138.5	Bureau		
	MEL180				PEER, Mel Canyon Rd	Landers Earthquake	0.23 36.93
Shallow Background	ABY090	EW [0°-60°]	7.3	75.2	PEER, Amboy	Landers Earthquake	0.245 49.98
	ABY000	NS [0°-60°]					0.251

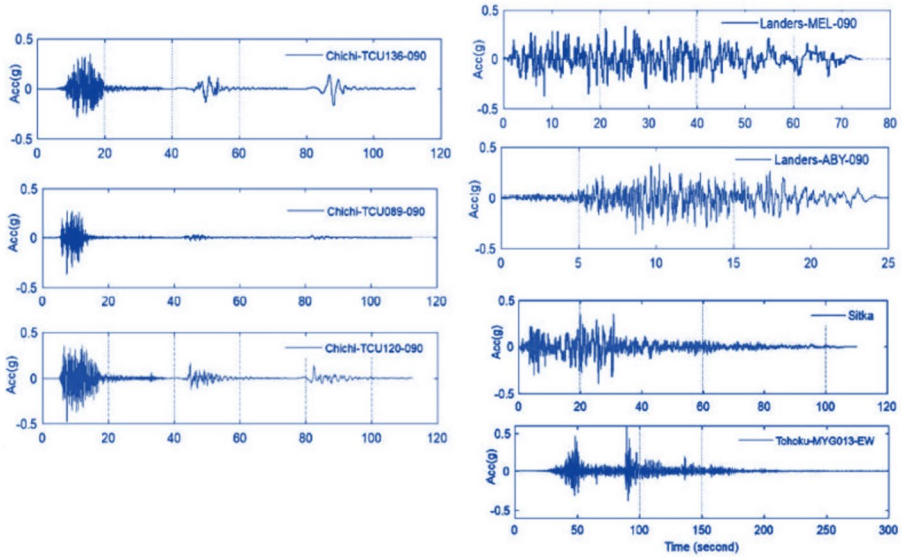


Fig. 10 Set of ground motion records used for the non-linear time history analysis (NLTHA)

shallow background mechanisms must be used for the study. This requirement describes the features of Indonesia’s earthquake source zones, which can be broadly categorized into three types: diffuse seismic zones, which are areas where earthquakes occur that are not connected to any particular fault or type of fault, strike-slip earthquakes along defined faults, and subduction events, which occur when an oceanic plate subducts beneath an island arc or continent (megathrust earthquake). Based on the aforementioned standards, seven pairs of ground motion are chosen for this investigation. Regrettably, due to a lack of seismic instrumentation in Indonesia, ground motions recorded meeting the aforementioned requirements are not available, hence past time histories

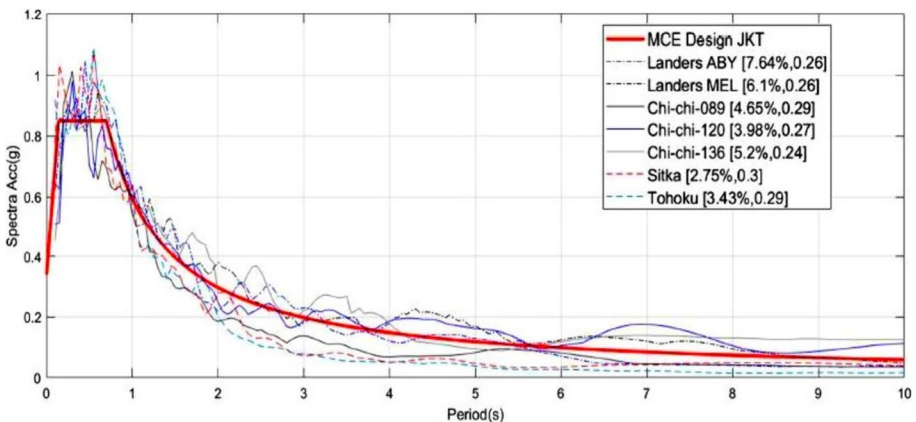


Fig. 11 Scaling of ground motions records in relation to the target response spectrum

of earthquakes in other nations with comparable conditions are used instead. They have a damping ratio of 5% and are adjusted to match the required response spectrum. 0.2 to 1.5 times the period at the first mode is the interval period of spectral matching. The east–west and north–south directions of the ground motions are carried out in a manner that is parallel to and perpendicular to the building plan, respectively. Table 3 and Fig. 10 provides specifics on the ground motions that were utilized in this investigation along with their attributes. The spectral-matched historical ground motion data utilized in the nonlinear time history analysis investigation are displayed in Fig. 11. The response spectra of seven historical ground motions are matched to the design response spectra for the maximum considered earthquake in Padang. Aside from that, factors such soil types, peak ground acceleration, distance from faults, and expected major event magnitudes all play a role in deciding which strong ground movements to implement. Selection of the robust ground motion records necessitates consideration of these characteristics.

Table 3 contains a tabulation of the seven pairs of ground motion recordings that were taken into consideration for this study. These records were obtained from the Pacific Earthquake Engineering Research (PEER) (PEER, 2016) database and were tabulated to comply with the minimum standards of the international codes.

6 Criteria for selecting the quantification controlling measures for seismic performance

6.1 Intensity measure (IM)

Scientists use the IM, or intensity measure, as an indicator to quantify earthquake susceptibility and evaluate earthquake records in IDAs. The quality of the IM can determine a

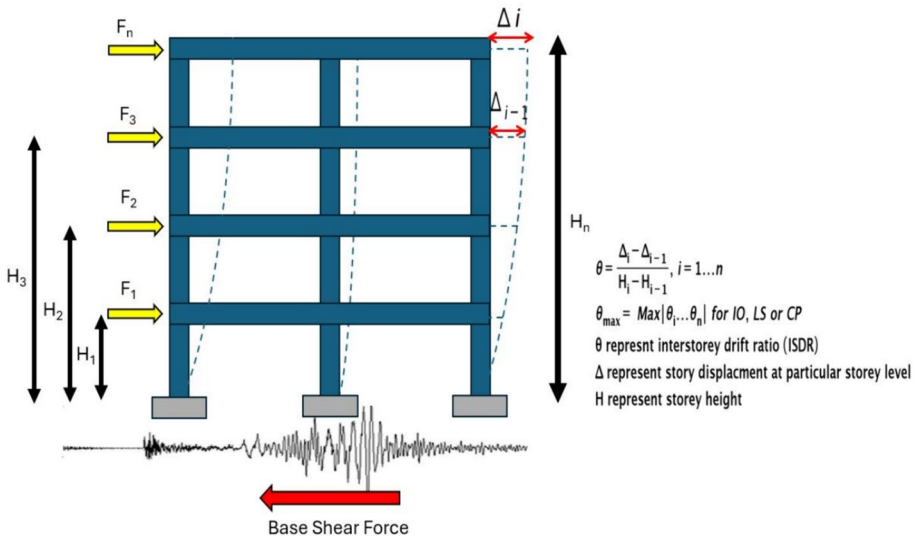


Fig. 12 2D frame prototype representation of the ISDR as an IM

structure’s vulnerability to ground vibrations and impact the precision and reliability of PSDMs. Researchers have offered various potential IMs such as PGA, PGV, Sa(T1), and A_I . As such, PGA was chosen as the critical IM in this study.

6.2 Damage measure (DM)

In fragility analysis and design, it is vital to establish a Damage Measure (DM) that accurately assesses the level of seismic damage in structures. A proficient DM should precisely depict the structural dynamic response caused by seismic action excitation. The most commonly employed DMs include maximum base shear, peak roof drift, peak floor acceleration and inter-story drift. Inter-story drift has been found to be more significantly related to structural deterioration than other measures of damage. For this research study, Kassem et al. (2023) demonstrated the efficacy of using Inter-Storey Drift Ratio (ISDR) as a DM making it an appropriate choice for measuring structural degradation induced by earthquakes as illustrated in Fig. 12 and represented in Eq. (20).

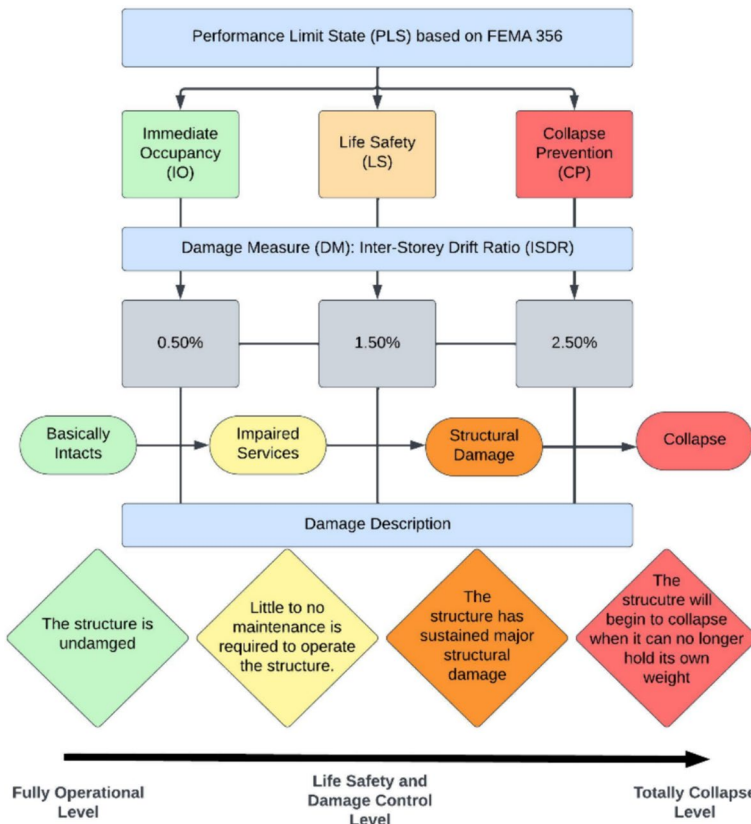


Fig. 13 The relationship between the description of damage and the stages of limitation according to FEMA 356

$$\% \theta = \frac{\Delta_i - \Delta_{i-1}}{H_i - H_{i-1}} \times 100 \quad (20)$$

where $\% \theta$ represents the inter-story drift ratio (ISDR), Δ represents the story displacement at particular story level, and H represents the story height.

6.3 Performance limit states according to FEMA 356

To be effective, it is necessary to have several limit states referred to as performance levels that accurately represent the structural damage condition during an earthquake. In this study, three limit states for the selected structure are defined according to FEMA 356: Immediate Occupancy (IO), Life Safety (LS) and Collapse Prevention (CP). These distinct limit state ranges were previously established at 0.5%, 1.50% and 2.50%, respectively, which were taken into account from FEMA356. Figure 13 shows the conceptual link between damage description and limit states employed in this study.

7 Conducting incremental dynamic analysis and evaluating the fragility of the structure

IDA, or Incremental Dynamic Analysis, is a methodology used to assess the structural behaviour in response to specific earthquake records. The process involves constructing a single curve for each ground motion, representing a particular damage measure (such as interstory drift), plotted against a specified intensity measure of the ground motion (such as peak ground acceleration, PGA). The primary goals of IDA are to enhance comprehension of the correlation between ground motion records and structural reaction, particularly in terms of the possible level of ground motion and the intensity of factors such as maximum displacement, strength, and stiffness. This approach has been extensively employed by numerous scholars in the analysis of nonlinear dynamics (Kassem et al. 2022a; Kassem et al. 2022b; and Ozturk 2017). The IDA curves are displayed by plotting the IM (Intensity Measure) of the PGA (Peak Ground Acceleration) in relation to the EDP (Engineering Demand Parameter) of the %ISDR (Interstory Drift Ratio) to offer a comprehensive perspective of the seismic performance dependent on the level of damage reached.

Afterward, the fragility can be defined as a possibility of experiencing damage equal to or greater than a certain state. Seismic parameters including spectral acceleration, spectral displacement, peak ground velocity, and PGA are used to express it (Kumitani and Takada 2009; Kirçil and Polat 2006; Duan and Pappin 2008). See, for instance, (HARAN et al. 2015, Silva et al. 2014, Bakhshi and Asadi 2013; Modica and Stafford 2014; Frankie et al. 2013), where some scholars have offered historical context about the evolution of the fragility curves. One can construct fragility curves using one of four methods: the expert-based or judgmental method, which relies on expert estimates and opinions; the empirical method, which uses damage data reported from past earthquakes, the analytical method, which relies on time history analyses; and the hybrid method, which combines experimental and numerical analysis. Each approach was outlined, with benefits and drawbacks, by Muntasir Billah and Shahria Alam (2015). The analytical method is the most popular because it does not necessitate experimental or damage data, unlike the other methods as

provided in this study. Among the analytical methods, the Ibrahim and El-Shami (2011) method is one of the simplest. Equation (21) defines the conditional likelihood of a structure reaching or exceeding a specified damage state (DS), given the PGA, in this method:

$$P(DS/PGA) = \phi\left(\frac{\ln(PGA) - \mu}{\sigma}\right) \quad (21)$$

Let represent the ϕ standard normal cumulative distribution function. and represent the μ mean value and σ standard deviation of the natural logarithm of PGA when the building achieves a given damage state or performance level, D .

Equation (21) was derived from the research conducted by Shinozuka et al. (2000). In their study, they constructed analytical fragility curves by employing nonlinear dynamic analysis (NLDA). These fragility curves were expressed using two-parameter lognormal distribution functions, which were determined using the procedure known as maximum likelihood. The fragility curve is also known as a probabilistic approach and computed via cumulative distribution function (CDF) by dividing the total number of data points obtained from the IDA analysis by the number of data points that reached or surpassed a specific damage state. Besides, the investigation was conducted to assess the accuracy of utilizing the mean and standard deviation parameters.

A crucial aspect in the development of the fragility function is the identification and precise definition of the appropriate damage states. The engineering demand parameter (EDP) utilized for evaluating the structure being studied is the maximum inter-storey drift ratio (ISDR_{max}). This value acts as a measurable global indication of the deterioration status in the structures.

The literature has outlined three distinct damage states/performance levels: immediate occupancy (IO), life safety (LS), and collapse prevention (CP). The performance levels are determined by a specific measure of damage, primarily the interstorey drift ratios (expressed as percentages). The maximum permissible interstorey drifts for each performance level may vary as they are contingent upon the expert's discretion. The recommendations of FEMA 356 are frequently utilized (see Fig. 13).

8 Results and discussion

8.1 Evaluation of structural response through incremental dynamic analysis and regression analysis: investigating the interplay among orientation (θ), intensity measures (IM), and structural behavior (SB)

Recognizing the structural behavior of a chosen structural system is essential when confronted with diverse ground movements from various directions, particularly if the system was constructed without considering specific seismic design regulations. To assess the seismic performance of the chosen structure in Padang while taken into account earthquake multi-directional angles indicated in the X, Longitudinal Direction (E–W) and the Y, Transverse Direction (N–S), ranging from 0° to 60° in increments of 15°. A Nonlinear Time History Analysis (NL-THA) embodied by Incremental Dynamic Analysis (IDA) is employed, by utilizing the performance limit states stipulated by FEMA 356 and the recommendations made by the Performance-Based Earthquake Engineering (PBEE) framework. Incremental dynamic analysis is a quantitative method that assesses the most

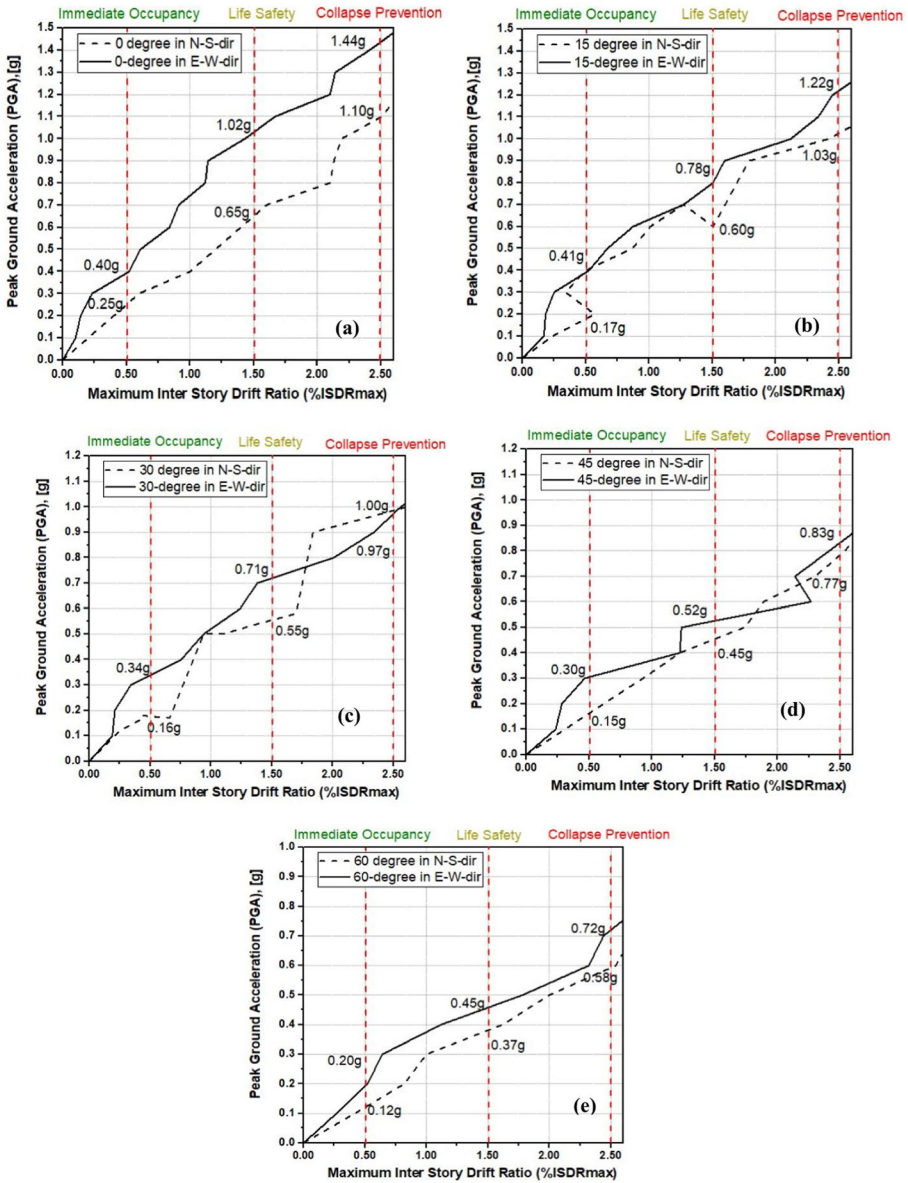


Fig. 14 Incremental dynamic analysis curves for ground motions with varied incidence angles in the x and y directions

crucial factors influencing a structure’s performance and seismic capacity as illustrated in Figs. 14a–e and 15, and Table 4 displays the intensity measure for each angle of incidence with respect to PLS, as well as the percentage difference represented by the structural behavior (S_B) when subjected to an earthquake in the east–west and north–south directions.

Seismic structural behavior analysis is crucial in ensuring the resilience and safety of built environments against earthquake events. A detailed examination of the provided

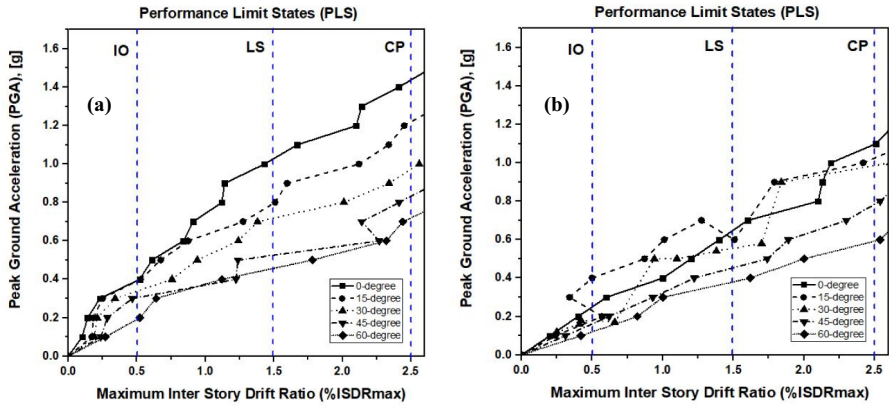


Fig. 15 Composite capacity curves for structures subject to multidirectional incidence angles along east-west (E–W) and north-south (N–S) axes

data, focusing on the variations in structural behavior (S_B) across different intensity measures, angles of incidence, and their implications for structural design. The IDA curves are graphed by plotting the IM of the PGA (g) against the EDP of the ISDR. This is done to give a comprehensive assessment of the selected structural building against multiple seismic excitations with different angle of incidence (0° to 60°) and directions (E–W and N–S) and different seismic scenarios (produced by the megathrust, Benioff, shallow crustal, and shallow background mechanisms) to the point of collapse and other damage states, as seen in Figs. 14 and 15 and summarized in Table 4.

Beginning with the angle of incidence ($\theta=0^\circ$) chosen as a controlled angle to provide the clarity of the results (This serves as the fundamental point of reference for comparison). Based on the results, it was found that in the direction of (N–S), represented by the Y-directional component, 0.25g is needed to attain the IO performance level, whereas in the direction of (E–W), represented by the X-directional component, 0.41g is required. That, in turn, implies the structure is serving its purpose continuously with very little degradation. There can be some small cracks in the frame’s structural components. Furthermore, 0.65g was needed for the direction of (N–S) ground motions movements and 1.02g was needed for the direction of (E–W) ground motions movements to attain the LS performance level. Despite the fact that this level may not pose significant dangers of falling debris within or outside the structure, it does cause significant damage to a few frame components due to the residual strength and stiffness that persists in all levels of the building. Moreover, at the CP performance level, both seismic situations (N–S) and (a) necessitate acceleration values of 1.10 g and 1.40 g, respectively. The structure is on the point of complete collapse as a result of significant deterioration in the strength and rigidity of the system that resists lateral forces, as well as extensive permanent deformation of the structure. Consequently, there is a possibility that the structure may be irreparable and unsafe for reconstruction.

Based on the directional dependency with ($\theta=0^\circ$), there is a distinct variation in the structural response between the north-south and east-west directions. This indicates that the behaviour of the structure is greatly affected and influenced by the orientation of the ground movement. The ground motion intensity, expressed as acceleration relative to gravity (g), is represented by the values of 0.25g, 0.65g, and 1.10g for drift ratios of 0.50%,

Table 4 Comparative analysis of intensity measures for various incidence angles with respect to pseudo-lateral strength: percentage differences in structural performance under earthquake impact in east–west and north–south directions

Angle of Incidence (θ)	Intensity Measure in N–S direction	Intensity Measure in E–W direction	% Structural Behavior (S_p) difference during GMs in (N–S and E–W dirs.)	% Structural Behavior (S_p) between Angle of Incidence (θ) controlled by 0° (N–S dir.)	% Structural Behavior (S_p) between Angle of Incidence (θ) controlled by 0° (E–W dir.)
<i>IM at ISDR = 0.5% of IO limit</i>					
0°	0.25	0.41	37.50%	(Controlled by 0°)	(Controlled by 0°)
15°	0.17	0.40	58.50%	– 32.0%	– 2.40%
30°	0.16	0.34	52.90%	– 36.0%	– 17.00%
45°	0.15	0.30	50.00%	– 40.0%	– 26.83%
60°	0.12	0.20	40.00%	– 52.0%	– 51.20%
<i>IM at ISDR = 1.50% of LS limit state</i>					
0°	0.65g	1.02g	36.00%	(Controlled by 0°)	(Controlled by 0°)
15°	0.60g	0.78g	23.10%	– 7.70%	– 23.53%
30°	0.55g	0.71g	22.53%	– 15.40%	– 30.39%
45°	0.45g	0.52g	13.46%	– 30.77%	– 49.02%
60°	0.37g	0.45g	17.77%	– 43.10%	– 55.88%
<i>IM at ISDR = 2.50% of CP limit state</i>					
0°	1.10g	1.40g	21.42%	(Controlled by 0°)	(Controlled by 0°)
15°	1.03g	1.22g	15.57%	– 6.30%	– 12.85%
30°	1.00g	0.97g	3.00%	– 9.10%	– 30.71%
45°	0.77g	0.83g	7.23%	– 30.00%	– 40.71%
60°	0.58g	0.72g	19.44%	– 47.30%	– 48.57%

From the given data, we can observe the following trends: As the angle of incidence increases (θ), the structural behavior is reduced. As the angle of incidence increases, the intensity measure generally decreases and reaches the damage state. 0° Angle of Incidence (Control): This serves as the baseline reference for comparison. At this angle, the structural behavior is relatively stable, providing a benchmark for evaluating the effects of variations in angle of incidence

1.50%, and 2.50%, respectively. In the N–S direction, the values are 0.41 g, 1.02 g, and 1.40 g for the same drift ratios in the E–W direction. The values in the north–south direction continuously exhibit much lower magnitudes compared to those in the east–west direction, indicating a notable effect of (37.50%, 36.0%, and 21.42%) on the structural behaviour for IO, LS, and CP damage states. However, when considering the angle incidence dependency, it shows similar influence, when the angle of incidence increases from ($\theta=0^\circ$) to ($\theta=60^\circ$) with an increment of 15° it is observed that the impact of earthquakes in north–south reaches the optimum of their limit states earlier than the earthquakes in east–west direction. For instance, at CP limit state, the structure collapses at 0.58g when exposed to an orientation of ($\theta=60^\circ$) in (N–S) directions, whereas in (E–W) direction, collapse occurs at 0.72g. This indicates that the structure's response to ground motion is significantly influenced by both the angle of incidence and the directional characteristics of the ground motion. In addition, this comparison between directionality and incidence control helps to learn how the structure's react changes concerning the N–S and E–W directions as the angle of incidence deviates from the reference angle (0°). As the angle of incidence increases, the structural response becomes increasingly asymmetric, with larger differences in acceleration between the N–S and E–W directions. This underscores the need for designers to account for directional effects when assessing the seismic performance of structures.

Besides, the analysis reveals distinct trends in structural behavior (S_B) concerning intensity measures and angles of incidence. Firstly, as the intensity measure increases, the structural behavior exhibits a clear trend of deterioration. This aligns with fundamental principles in seismic engineering, where higher intensity ground motions lead to more severe structural responses due to increased forces and deformations. Furthermore, the angle of incidence plays a significant role in influencing structural behavior. Generally, as the angle of incidence increases, the structural behavior tends to worsen. This can be attributed to the changing dynamic response of structures to ground motions arriving from different angles, resulting in variations in stress distributions and deformation patterns. Interestingly, the percentage difference in structural behavior decreases as the angle of incidence increases from 0° to 60° . An explanation for this might be that when the angle of incidence increases, the structure's strength and rigidity decrease, making it less equipped to resist earthquakes in both directions. For instance, when the angle of incidence is 60° , the structural behavior (S_B) loses about half of its tolerance for lateral motion in all damage states until it reaches its collapse state in both the N–S and E–W directions.

Comparisons across different intensity measures further highlight the sensitivity of structural behavior to seismic loading conditions. At lower intensity measures, the structural behavior shows moderate levels of deterioration, while at higher intensity measures, the deterioration becomes more pronounced, particularly at larger angles of incidence.

Additionally, comparisons across angles of incidence demonstrate consistent trends of worsening structural behavior as the angle increases. This underscores the importance of accounting for angle of incidence effects in structural analysis and design, as structures may experience more severe responses under oblique ground motions. These findings have significant implications for structural design and assessment. Designers must carefully consider directional effects and angle of incidence variations when evaluating structural behavior under seismic loading. Differential responses between different directions may necessitate tailored design approaches to ensure uniform performance across all loading scenarios.

Furthermore, the sensitivity of structural behavior to intensity measures underscores the importance of accurate seismic hazard assessments in design practices. By incorporating these findings into design methodologies and guiding future research endeavors, we can contribute to the development of more resilient and sustainable built environments capable of withstanding seismic events effectively.

Meanwhile, the regression analysis offers a systematic approach to investigate the complex interactions between various factors (θ vs. IM) and (θ vs. S_B) influencing structural building performance under multiple direction of earthquake loading. By identifying key variables and quantifying their relationships, this analytical framework contributes to the development of evidence-based strategies for enhancing seismic resilience in the built environment. By examining these variables, engineers and policymakers can make informed decisions regarding design specifications, construction materials, and retrofitting strategies to enhance building resilience. The two factors that regulate the structural seismic response are (θ vs. IM) and (θ vs. S_B) correlated the R-square coefficient for the correlation and the polynomial equations as illustrated in Figs. 16a–c and 17a–c and Table 5.

From the results obtained, the correlation between structural building characteristics (S_B) and intensity measures (IM) with respect to the angle theta (θ) is a crucial aspect in earthquake engineering, as it helps understand how the orientation of ground motion influences the response of buildings. The provided R-square values represent the strength of the correlation between two variables: the Angle of Incidence (θ) and Intensity Measures (IM), and the Angle of Incidence (θ) and Structural Behavior (S_B). These correlations are analyzed separately for different ground motion conditions and directions.

The R-square values for both Intensity Measures (IM) and Structural Behavior (S_B) correlations at Immediate Occupancy (IO) in North–South (N–S) and East–West (E–W) directions are notably high, indicating robust correlations between the Angle of Incidence (θ) and both IM and S_B during ground motions in both orientations. Notably, the correlation tends to be marginally stronger in the E–W direction compared to the N–S direction for both IM and S_B . Similarly, at Life Safety (LS) conditions, the R-square values remain very high for both N–S and E–W directions, suggesting exceptionally strong correlations between θ and IM as well as S_B , with the correlation slightly stronger compared to IO. Collapse Prevention (CP) conditions exhibit similarly high R-square values for both IM and S_B correlations in both N–S and E–W directions, with S_B displaying an especially strong correlation, almost reaching 1.0. Notably, the correlation between θ and IM is marginally stronger at CP compared to LS and IO for both orientations.

Overall, these high R-square values indicate that the Angle of Incidence (θ) is strongly correlated with both Intensity Measures (IM) and Structural Behavior (S_B) during ground motions, across different ground motion conditions and directions. This suggests that θ is a significant factor influencing building responses to seismic events, and understanding its relationship with IM and S_B is essential for seismic risk assessment and mitigation strategies.

Moreover, from the provided fitting equations for the relationship between the Angle of Incidence (θ) and Intensity Measures (IM) and Structural Behavior (S_B) the fitting equations allows us to understand the quantitative relationships between θ , IM, and S_B , providing valuable insights into structural behavior under varying angles of incidence and intensity measures. These insights can inform structural design, risk mitigation strategies, and decision-making processes in earthquake-prone regions.

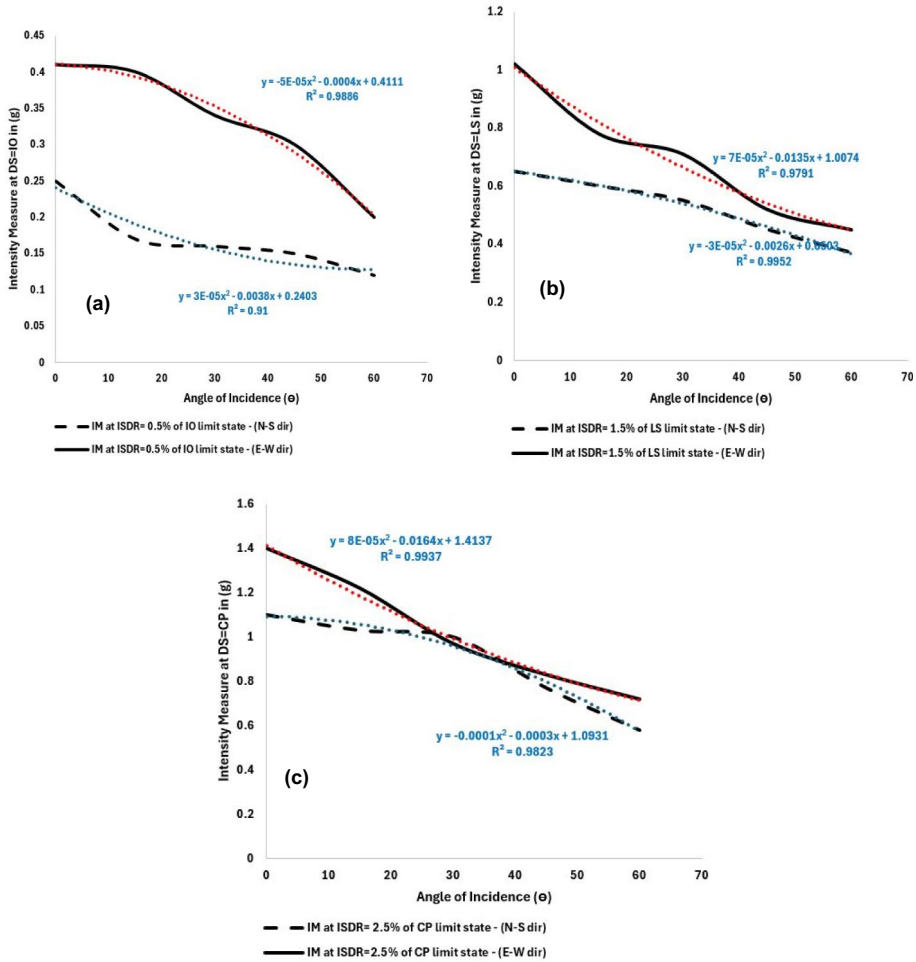


Fig. 16 Regression analysis of the three performance limit states (IO, LS, and CP) as a function of angle of incidence (θ) and intensity measure (IM) in east–west (E–W) and north–south (N–S) directions

8.2 Generalized equation using regression analysis, and providing their coefficients

To derive a general equation that describes the relationship between the Angle of Incidence (θ) and Intensity Measures (IM) in both the North–South (N–S) and East–West (E–W) directions, a polynomial regression is utilized using Python as shown in Fig. 18. The availability of IM data points collected at different incidence angles allows to fit the data using a polynomial equation.

The N–S and E–W directions will be addressed independently in order to fit a polynomial equation for IM.

For N–S direction: Let $IM_{N-S}(\theta)$ be the Intensity Measure in the N–S direction.

The polynomial equation:

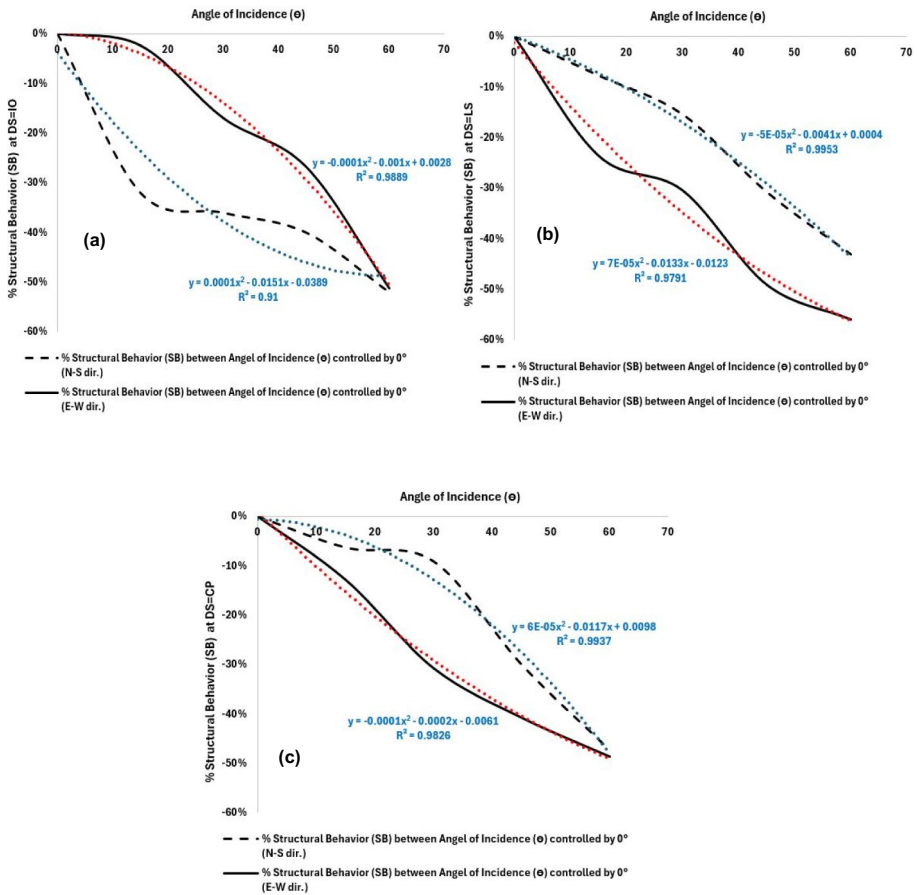


Fig. 17 Regression analysis of the three performance limit states (IO, LS, and CP) as a function of angle of incidence (θ) and structural behavior (S_B) in east–west (E–W) and north–south (N–S) directions

$$IM_{N-S}(\theta) = a_0 + a_1\theta + a_2\theta^2 \tag{22}$$

Similarly, for the E–W direction:

For E–W direction: Let $IM_{E-W}(\theta)$ be the Intensity Measure in the E–W direction.

The polynomial equation:

$$IM_{E-W}(\theta) = b_0 + b_1\theta + b_2\theta^2 \tag{23}$$

Although, to derive a general equation that describes the relationship between the Angle of Incidence (θ) and Structural Behavior (SB) in both the North–South (N–S) and East–West (E–W) directions, a polynomial regression is utilized. The availability of S_B data points collected at different incidence angles allows to fit the data using a polynomial equation.

For N–S direction: Let $SB_{N-S}(\theta)$ be the Intensity Measure in the N–S direction.

Table 5 Regression analysis and fitting equations for correlating two variables with respect to the angle of incidence

Damage States/ Dir	R-square (θ vs. IM)	R-square (θ vs. S _B)	Fitting Equation (θ vs. IM)	Fitting Equation (θ vs. S _B)	Remark
At IO/(N-S)	0.91	0.91	$IM_{N-S}(\theta) = 3E-05\theta^2 - 0.0038\theta + 0.2403$	$SB_{N-S}(\theta) = 0.0001\theta^2 - 0.0151\theta + 0.0389$	The (IM and SB) variables strongly correlate with (θ)
At IO/(E-W)	0.9886	0.9889	$IM_{E-W}(\theta) = -5E-05\theta^2 - 0.0004\theta + 0.4111$	$SB_{E-W}(\theta) = -0.0001\theta^2 - 0.001\theta + 0.0028$	The (IM and SB) variables strongly correlate with (θ)
At LS/(N-S)	0.9952	0.9953	$IM_{N-S}(\theta) = -3E-05\theta^2 - 0.0026\theta + 0.0503$	$SB_{N-S}(\theta) = -5E-05\theta^2 - 0.0041\theta + 0.0004$	The (IM and SB) variables strongly correlate with (θ)
At LS/(E-W)	0.9791	0.9791	$IM_{E-W}(\theta) = 7E-05\theta^2 - 0.0135\theta + 1.0074$	$SB_{E-W}(\theta) = 7E-05\theta^2 - 0.0133\theta - 0.0123$	The (IM and SB) variables strongly correlate with (θ)
At CP/(N-S)	0.9823	0.9937	$IM_{N-S}(\theta) = -0.0001\theta^2 - 0.0003\theta + 1.0931$	$SB_{N-S}(\theta) = 6E-05\theta^2 - 0.0117\theta + 0.0098$	The (IM and SB) variables strongly correlate with (θ)
At CP/(E-W)	0.9937	0.9826	$IM_{E-W}(\theta) = 8E-05\theta^2 - 0.0164\theta + 1.4137$	$SB_{E-W}(\theta) = -0.0001\theta^2 - 0.0002\theta - 0.0061$	The (IM and SB) variables strongly correlate with (θ)

The polynomial equation:

$$SB_{N-S}(\theta) = c_0 + c_1\theta + c_2\theta^2 \tag{24}$$

Similarly, for the E–W direction:

For E–W direction: Let $SB_{E-W}(\theta)$ be the Intensity Measure in the E–W direction.

The polynomial equation:

$$SB_{E-W}(\theta) = d_0 + d_1\theta + d_2\theta^2 \tag{25}$$

The relationships between the Angle of Incidence (θ), Structural Behavior (S_B), and Intensity Measures (IM) are illustrated in these equations in both the N–S and E–W directions. It is possible to predict S_B and IM at any given (θ) angle using the values of the coefficients and their general equation, which are provided in Table 5, for each performance limit state of IO, LS, and CP.

```
# Importing necessary libraries
import numpy as np
import pandas as pd
from sklearn.preprocessing import PolynomialFeatures
from sklearn.linear_model import LinearRegression

# Given data
data = {
    'Angle_of_Incidence': [0, 15, 30, 45, 60],
    'Intensity_Measure_N-S': [0.25, 0.17, 0.16, 0.15, 0.12],
    'Intensity_Measure_E-W': [0.41, 0.40, 0.34, 0.30, 0.20]
}

# Creating a DataFrame
df = pd.DataFrame(data)

# Extracting features (Angle_of_Incidence) and targets (Intensity_Measure_N-S, I
X = df[['Angle_of_Incidence']]
y_M_S = df['Intensity_Measure_N-S']
y_E_W = df['Intensity_Measure_E-W']

# Polynomial regression degree
degree = 2

# Polynomial features transformation
poly_features = PolynomialFeatures(degree=degree)
X_poly = poly_features.fit_transform(X)

# Polynomial regression model
model_M_S = LinearRegression()
model_E_W = LinearRegression()

# Fitting the models
model_M_S.fit(X_poly, y_M_S)
model_E_W.fit(X_poly, y_E_W)

# Predicting values
X_pred = np.linspace(0, 60, 100).reshape(-1, 1)
X_pred_poly = poly_features.transform(X_pred)
y_pred_M_S = model_M_S.predict(X_pred_poly)
y_pred_E_W = model_E_W.predict(X_pred_poly)

# Print the coefficients
print('Coefficients for N-S direction', model_M_S.coef_)
print('Coefficients for E-W direction', model_E_W.coef_)
```

(a)

```
# Importing necessary libraries
import numpy as np
import pandas as pd
from sklearn.preprocessing import PolynomialFeatures
from sklearn.linear_model import LinearRegression

# Given data
data = {
    'Angle_of_Incidence': [0, 15, 30, 45, 60],
    'SB_N-S': [0, -32.0, -36.0, -40.0, -52.0],
    'SB_E-W': [0, -2.40, -17.00, -26.83, -81.20]
}

# Creating a DataFrame
df = pd.DataFrame(data)

# Extracting features (Angle_of_Incidence) and targets (SB_N-S, SB_E-W)
X = df[['Angle_of_Incidence']]
y_SB_N_S = df['SB_N-S']
y_SB_E_W = df['SB_E-W']

# Polynomial regression degree
degree = 2

# Polynomial features transformation
poly_features = PolynomialFeatures(degree=degree)
X_poly = poly_features.fit_transform(X)

# Polynomial regression model
model_SB_N_S = LinearRegression()
model_SB_E_W = LinearRegression()

# Fitting the models
model_SB_N_S.fit(X_poly, y_SB_N_S)
model_SB_E_W.fit(X_poly, y_SB_E_W)

# Predicting values
X_pred = np.linspace(0, 60, 100).reshape(-1, 1)
X_pred_poly = poly_features.transform(X_pred)
y_pred_SB_N_S = model_SB_N_S.predict(X_pred_poly)
y_pred_SB_E_W = model_SB_E_W.predict(X_pred_poly)

# Print the coefficients
print('Coefficients for SB_N-S', model_SB_N_S.coef_)
print('Coefficients for SB_E-W', model_SB_E_W.coef_)
```

(b)

Fig. 18 Polynomial regression and modal fitting analysis via Python: a intensity measure (IM) vs. angle of incidence (θ), and b structural behavior (SB) vs. angle of incidence (θ)

8.3 Fragility and collapse margin ratio for different angle of incidence

The seismic performances of the select RC frame structure under set of ground motion records with different angle of incidence (0° to 60°) and different orientations in (E–W) and (N–S) were determined using fragility curves by recording the damage for three performance limit states (IO, LS, and CP) in terms of possibilities of damages at different intensity measures as shown in Fig. 19. The results provide the probability of damage at various peak ground accelerations (PGA) for different angles of incidence (θ) and directions (E–W and N–S). At intensity measure $0.6g$ which is considered the maximum considered earthquake (MCE_G) intensity based on 2017 national seismic hazard maps of Indonesia is chosen for analyzing the outcomes, that was developed by probabilistic approach for 2% probability of exceedance in 50 years as shown in the PGA map in Fig. 20.

Starting with the E–W directional component at angles of ($\theta = 15^\circ, 30^\circ, 45^\circ, \text{ and } 60^\circ$) for the CP limit state, the probability of damage upon reaching or beyond the CP state is (50%, 55%, 60.50%, 65.34%), accordingly. On the other hand, the probability of damage for reaching or exceeding the CP state is (69.15%, 76.06%, 83.67%, 90.3%), respectively, on the N–S directional component. At a controlled angle of 0° , the probability of damage for both the east–west and north–south directions of ground motion is 50%, as tabulated in Table 6. However, when the intensity measure goes beyond $0.6g$, the likelihood of damage for the north–south direction gets higher than that for the east–west. For example, at $0.7g$, the likelihood of damage for the north–south direction reaches 84%, while for the east–west it reaches 69%. The possibility of damage is much higher in the N–S direction compared to the E–W direction for the same PGA and angle of impact. This indicates that building can be more susceptible to seismic pressures when they occur in a north–south orientation. This implies that the structure may be more vulnerable to seismic forces in the N–S direction. Besides, an increase in the angle of incidence leading to a noticeable effect on the probability of damage. The general pattern of a higher probability of destruction as PGA values increase is consistent regardless of the angle of impact.

For the immediate occupancy level, and in the case of an earthquake, it is essential to keep a close eye on the occupancy levels of buildings since these are considered to be of significant importance. As the intensity measures approach $0.35g$ and $0.4g$, it is evident that the building rapidly loses their occupancies. This is because the structure has the potential to sustain damage that is total in-occupant of 100%.

As an additional point of interest, the life safety of a structure is put in risk during seismic occurrences, and this stage is regarded to be a crucial step following the structure occupancy stage since it may assist in determining the extent to which repairs are required. However, considering the 50% possibility of damage as half-life threatening structure is the key for monitoring the structure which needs an intensity range between $0.35g$ to $0.4g$ for both directions and all orientation angles except angle of 60° which requires a $0.17g$ during N–S ground motion. Meanwhile, the three performance levels, IO, LS, and CP, intersect at $1.0g$ for all seismic conditions, with a 100% damage potential.

This could signify that the structure may be stiffer to withstand earthquakes in the X-direction denoted by E–W compared to Y-direction denoted by N–S even if there is center of rigidity and center of mass for both X, and Y that reflect the stiffness of the structure are compatible as provided in Table 7. While the dynamic characteristics of the structure, such as natural frequencies and modes of vibration, may contribute to its stiffness in specific directions especially in this scenario: (1) Modal participation ratio for the X-direction is 99%, (2) Modal participation ratio for the Y-direction is 89%. Comparing the modal participation ratios, which

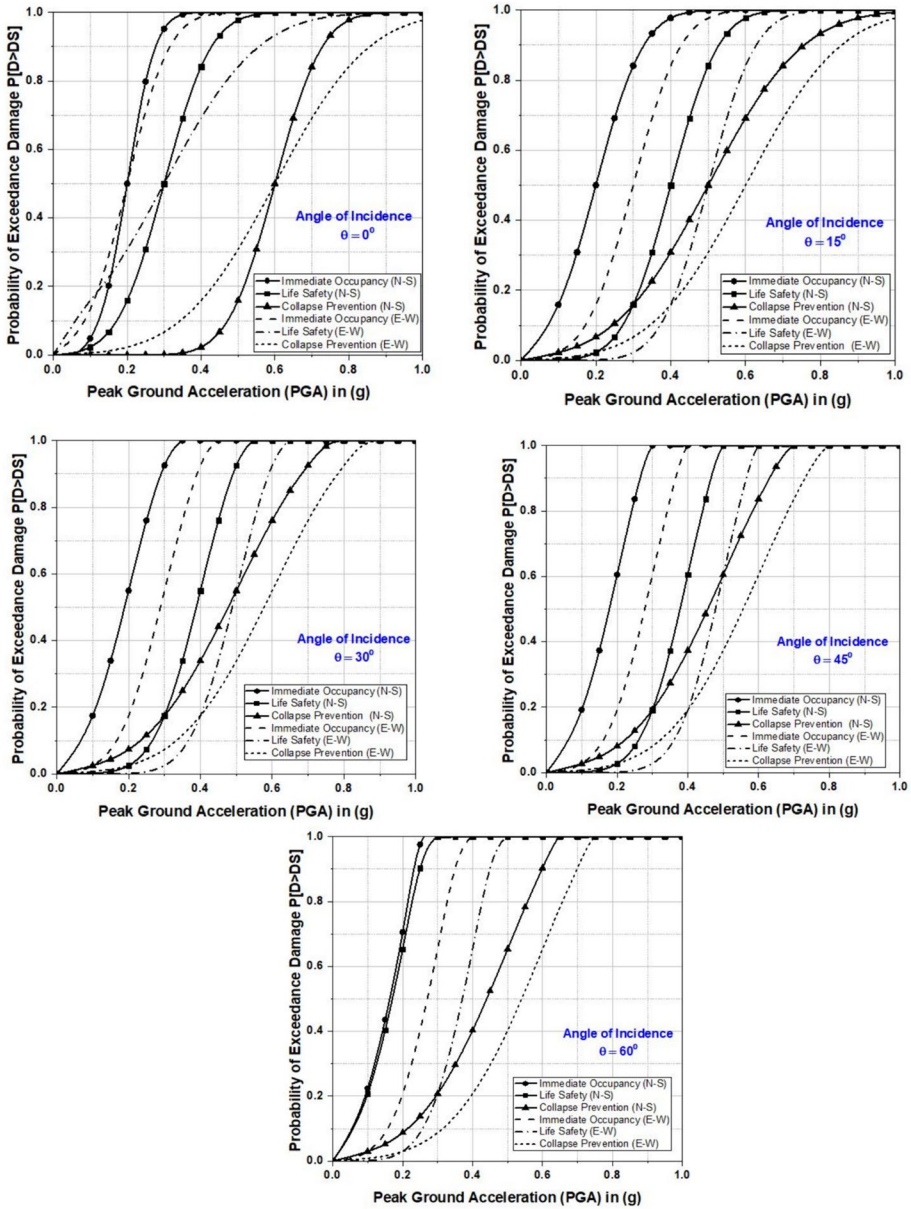


Fig. 19 Fragility curves depicting structural vulnerability for various seismic incident angles and directions for three performance limit states (PLS)

infer that the structure is stiffer in the X-direction. The higher modal participation ratio for the X-direction (99%) indicates that the modes associated with this direction contribute more significantly to the overall structural response, suggesting greater stiffness in the X-direction compared to the Y-direction. In addition, the relative magnitudes of the mode periods can also give insights into the dynamic behavior of the structure. This insight is crucial in seismic risk

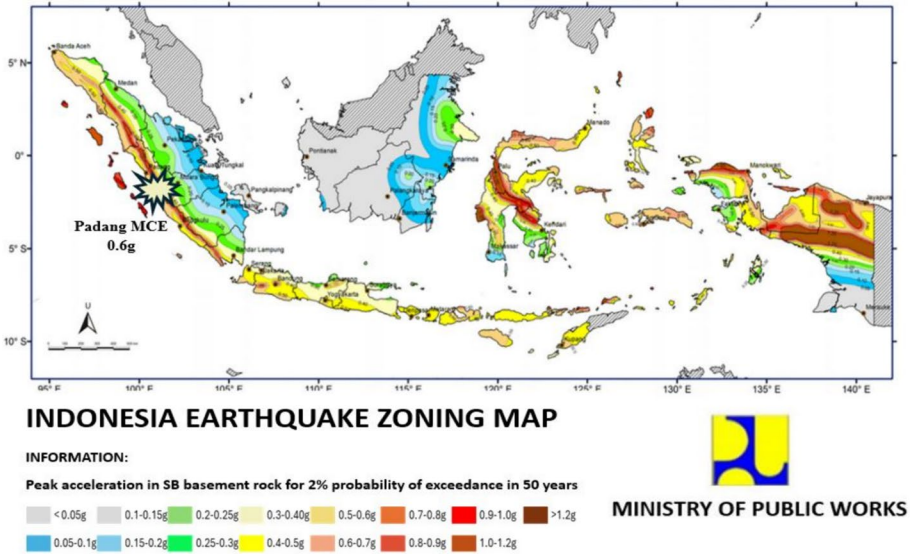


Fig. 20 Spatial distribution of peak ground acceleration (PGA) across Indonesia considering a 2% probability of exceedance in 50 years

Table 6 Probability of damages at MCE_G intensity measure for multi-angle of incidence and their directions during CP state

Angle of incidence (θ)	P[D/CP] at MCE _G in Case of E–W ground motion direction (%)	P[D/CP] at MCE _G in Case of N–S ground motion direction (%)
15°	50	69.15
30°	55.5	76.06
45°	60.50	83.67
60°	65.34	90.30

assessment and structural design, where ensuring adequate stiffness and response characteristics in both directions is essential for overall structural resilience. Engineers can improve structural performance and reduce risks by studying modal features and seismic loading responses. For example, if Mode 1 has a significantly longer period than Mode 2, it may dominate the structure’s response to certain types of dynamic loading or excitation, influencing factors such as resonance and damping. Therefore, the X-direction of the structure is more robust against seismic movements than the Y-direction, according to the dynamic characteristics given by the modal participation ratios and mode shape, as well as the seismic risk assessment derived from fragility and capacity curves. Figure 21 displays the selected model’s mode forms.

Moreover, the Collapse Margin Ratio (CMR) has been widely considered to be a very reliable seismic indicator of a building’s collapse safety since its release in FEMA P695. According to FEMA, it is the ratio of the ground motion intensity of the Maximum Considered Earthquake (MCE) to the median collapse intensity as estimated from a fragility curve. Equation (26) shows that the collapse margin ratio (CMR) is the ratio of the ground motion

intensity that corresponds to the 50% chance of structural collapse to the ground motion intensity that corresponds to the (MCE_G).

$$CMR = \frac{IM_{\%50P(D|CP)}}{IM_{MCE_G}} \tag{26}$$

where $IM_{\%50P(D|CP)}$ is the ground motion intensity corresponding to the 50% probability of structural collapse; IM_{MCE_G} is the ground motion intensity corresponding to the MCE level for the design. The MCE intensity used is 0.60 g according to the 2017 national seismic hazard maps of Indonesia-Padang.

According to the collapse margin ratio (CMR) initially proposed by FEMA P695, the intensity measure ($IM_{50\%}$) for reaching the 50% of the structural collapse for E–W directional component at angles of ($\theta = 15^\circ, 30^\circ, 45^\circ,$ and 60°) are (0.60 g, 0.57 g, 0.56 g, 0.53 g), respectively. However, for N–S directional component the ($IM_{50\%}$) are (0.50g, 0.48g, 0.47g, and 0.44g), respectively. As shown in Table 8 and schematically in Fig. 22’s fragility curves, the CMR values for E–W seismic situations are (1.0, 0.95, 0.93, 0.88), whereas for N–S excitations, they decrease to (0.83, 0.80, 0.78, 0.73). This implies that in case of N–S the structure is threatened by partially collapse (50%) or earlier compared to E–W records, as well the angle of incidence increases in both directions the structure vulnerability gets worse. The CMR score helps to recognize which is more significant to obtain a more vulnerable detections on the structures. As a result, the collapse rate of the structure under N–S ground motion excitation with different angle of incidence is lower than the E–W ground motion excitations, since the CMR of the E–W ground motion shows the highest value. Therefore, CMR can be a helpful seismic metric for evaluating the structure during earthquakes.

The CMR and the results of the IDA’s fragility study are in agreement. The analyses also show that the chosen RC frame building can withstand the required seismic performance or MCE, and that the structure is more likely to collapse when subjected to N–S ground motion excitation than when subjected to E–W excitation, even when the angle of incidence and its increments are varied.

Table 7 Center of mass and center of rigidity across all story levels

Story	Centers of mass and rigidity			
	XCM	YCM	XCR	YCR
	m	m	m	m
Ground Floor	70.9654	26.7598	79.5502	28.1812
1st Floor	80.4235	28.5225	80.0515	28.4213
2nd Floor	82.0728	29.6296	80.5162	28.657
3rd Floor	82.0728	29.6296	80.8743	28.7676
4th Floor	82.0728	29.6296	81.1663	28.7892
5th Floor	82.0728	29.6296	81.4064	28.7407
6th Floor	82.0575	28.945	81.596	28.6677
7th Floor	81.9344	16.9391	81.7127	28.1483
Roof Top	80.5	14.15	81.7095	26.8637

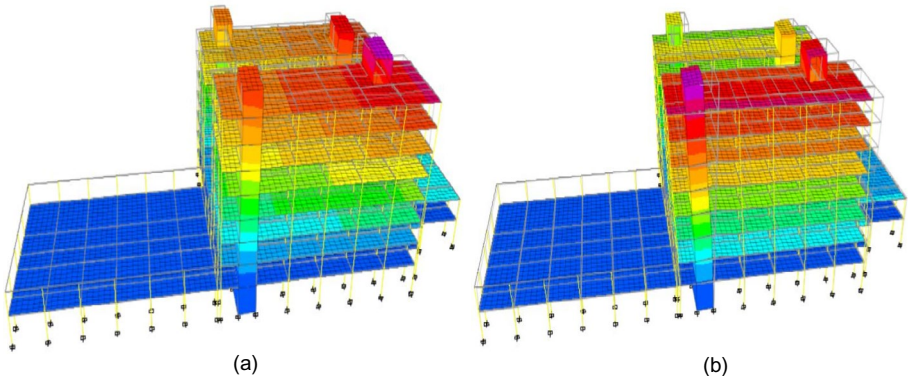


Fig. 21 Mode shapes of the analyzed structure: a mode 1 (Period=0.626 s), and b mode 2 (Period=0.583 s)

9 Conclusions

This study employs a probabilistic seismic demand model using fourteen ground motion records to assess the seismic vulnerability and response of a specific reinforced concrete (RC) frame structure in Padang, Indonesia. These records encompass seismic events such as Megathrust, Benioff, Shallow Crustal, and Shallow, analyzed across directional components north-south (N-S) and east-west (E-W) with angles of incidence ranging from 0° to 60° in 15-degree increments. Through Non-Linear Time-History Analysis (NL-THA) and Incremental Dynamic Analysis (IDA), this research identifies the structure’s capacity limit states as per FEMA 356, develops fragility functions, and calculates the Collapse Margin Ratio (CMR). Regression analysis, performed using Python, facilitated the derivation of a polynomial function specific to the model, yielding several key insights:

- (1) The IDA curve analysis provides a nuanced understanding of how structural behavior varies with intensity measures (IMs) and angles of incidence, demonstrating a decline in structural integrity with increasing IMs and incidence angles. This underscores the importance of considering directional and angular influences in seismic resilience assessments.
- (2) A significant correlation between structural behavior, intensity measures, and the angle of incidence was found, emphasizing the importance of these factors in earthquake engineering. The predictive model developed allows for accurate structural response estimations at any given incidence angle.
- (3) Fragility curves indicate a higher likelihood of damage in the north–south direction compared to the east–west, particularly under the same Peak Ground Accelerations (PGAs) and angles of incidence. This orientation-specific vulnerability and the sig-

Table 8 Comparative analysis of CMR values across three seismic scenarios

Seismic scenarios	IM _{MCE} (g)	IM _{50%} (g)	CMR
15° (E–W, N–S)	0.60	(0.6g, 0.5g)	(1.0, 0.83)
30° (E–W, N–S)	0.60	(0.57g, 0.48g)	(0.95, 0.8)
45° (E–W, N–S)	0.60	(0.56g, 0.47g)	(0.93, 0.78)
60° (E–W, N–S)	0.60	(0.53g, 0.44g)	(0.88, 0.73)

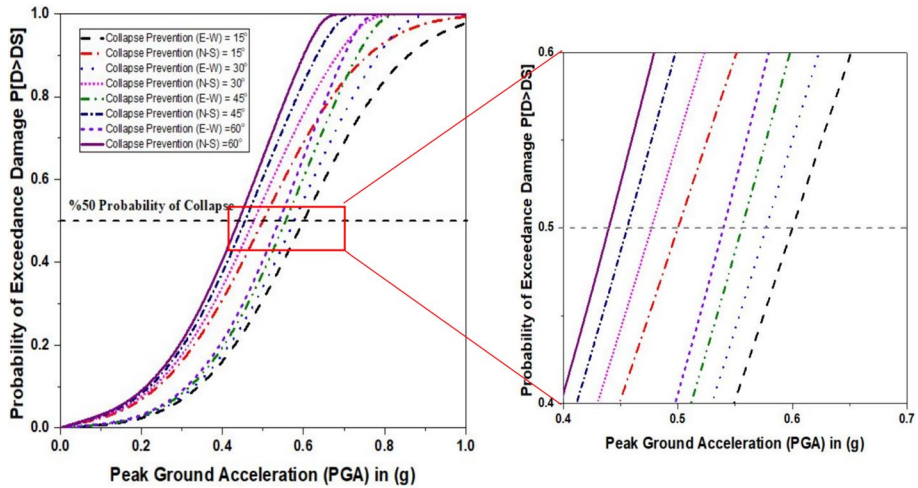


Fig. 22 Collapse fragility curves for structures subject to earthquake movements from multiple incident angles and orientations

nificant impact of the angle of incidence on damage probability highlight the need for tailored mitigation strategies.

- (4) The structure's dynamic characteristics suggest greater seismic resistance in the east–west direction (X-direction) than in the north–south (Y-direction), attributed to differences in modal participation ratios and dynamic properties. This implies the necessity of directional considerations in structural design to optimize seismic resilience.
- (5) The CMR analysis reveals a lower collapse rate under east–west ground motion excitations compared to north–south directions, emphasizing the importance of directional and angular factors in seismic risk mitigation. The findings support the need to incorporate these considerations into structural design and assessment practices to enhance the sustainability and resilience of built environments against seismic challenges.

This research highlights the critical role of multidirectional seismic input consideration in structural analysis and design for enhanced seismic resilience. By emphasizing the differential impact of seismic forces based on direction and angle of incidence, it advocates for a comprehensive approach that incorporates these insights into design practices, aiming to foster the development of structures capable of withstanding seismic events with minimal environmental impact.

Eventually, the comparisons across different angles of incidence consistently show a tendency of deteriorating structural behaviour as the angle rises. This highlights the significance of considering angle of incidence effects in structural analysis and design, since structures might face more intense reactions when subjected to oblique ground vibrations. The discoveries have important consequences for structural design and evaluation. Designers need to rigorously analyse directional effects and changes in angle of incidence when assessing structure response to seismic forces. Varying reactions in different directions may require customized design strategies to guarantee consistent performance in all loading situations. By integrating these discoveries into design approaches and directing next research efforts, we may aid in creating more durable and eco-friendly constructed environments that can successfully endure seismic disasters.

Acknowledgements This research was supported by Ministry of Higher Education Malaysia for Transdisciplinary Research Grant Scheme (TRGS) with Project Code: TRGS/1/2022/USM/02/3/1.

Author contributions All authors contributed to the study conception and design. Conceptualization, methodology and analysis were performed by Moustafa Moufid Kassem and Fadzli Mohamed Nazri. Writing the original draft of the manuscript was written by Moustafa Moufid Kassem, and Zaid A. Al-Sadoon. Visualizing and supervision were performed by Fadzli Mohamed Nazri and Salmia Beddu. All authors have read and agreed to the version of the final manuscript.

Data availability The datasets generated during and/or analyzed during the current study are available from the corresponding author on reasonable request."

Declarations

Conflict of interest The authors declared no potential conflicts of interest with respect to the research, authorship, and/ or publication of this article.

References

- Akhoondzadeh M (2024) Investigation of the LAIC mechanism of the Haiti earthquake (August 14, 2021) using CSES-01 satellite observations and other earthquake precursors. *Adv Space Res* 73(1):672–684. <https://doi.org/10.1016/j.asr.2023.09.042>
- Alam Z, Sun L, Zhang C, Samali B (2022) Influence of seismic orientation on the statistical distribution of nonlinear seismic response of the stiffness-eccentric structure. Paper presented at the Structures <https://doi.org/10.1016/j.istruc.2022.03.042>
- Anastasiadis K, Avramidis I, Panetsos P (2002) Concurrent design forces in structures under three-component orthotropic seismic excitation. *Earthq Spectra* 18(1):1–17. <https://doi.org/10.1193/1.14630>
- ASCE (2017) Minimum design loads and associated criteria for buildings and other structures
- Atak B, Avşar Ö, Yakut A (2014) Directional effect of the strong ground motion on the seismic behavior of skewed bridges
- Athanatopoulou A (2005) Critical orientation of three correlated seismic components. *Eng Struct* 27(2):301–312. <https://doi.org/10.1016/j.engstruct.2004.10.011>
- Athanatopoulou A, Tsourekas A, Papamanolis G (2005) Variation of response with incident angle under two horizontal correlated seismic components. *WIT Trans Built Environ* 81:10
- Bakhshi A, Asadi P (2013) Probabilistic evaluation of seismic design parameters of RC frames based on fragility curves. *Sci Iran* 20(2):231–241. <https://doi.org/10.1016/j.scient.2012.11.012>
- Cantagallo C, Camata G, Spacone E (2012) The effect of the earthquake incidence angle on seismic demand of reinforced concrete structures. Paper presented at the Proceedings of the 15th World Conference on Earthquake Engineering, Lisboa, Portugal.
- Duan X, Pappin JW (2008) A procedure for establishing fragility functions for seismic loss estimate of existing buildings based on nonlinear pushover analysis. Paper presented at the 14th World Conference on Earthquake Engineering
- EC (2004) Eurocode 8: design of structures for earthquake resistance-part 1: general rules, seismic actions and rules for buildings. European Committee for Standardization, Brussels
- El-Betar SA (2018) Seismic vulnerability evaluation of existing RC buildings. *HBRC J* 14(2):189–197. <https://doi.org/10.1016/j.hbrj.2016.09.002>
- Essar MY, Wahdati S, O'Sullivan B, Nemat A, Blanchet K (2024) Cycles of disasters in Afghanistan: the urgent call for global solidarity. *PLOS Global Public Health* 4(1):e0002751. <https://doi.org/10.1371/journal.pgph.0002751>
- FEMA (2000). NEHRP recommended provisions for seismic regulations for new buildings and other structures, 2000 edition, part 1: provisions, prepared by the Building Seismic Safety Council for The Federal Emergency Management Agency (Report FEMA 356) Washington, DC.
- Fontara I-KM, Kostinakis KG, Manoukas GE, Athanatopoulou AM (2015a) Parameters affecting the seismic response of buildings under bi-directional excitation. *Struct Eng Mech* 53(5):957–979. <https://doi.org/10.12989/sem.2015.53.5.957>
- Frankie TM, Gencturk B, Elnashai AS (2013) Simulation-based fragility relationships for unreinforced masonry buildings. *J Struct Eng* 139(3):400–410. [https://doi.org/10.1061/\(ASCE\)ST.1943-541X.0000648](https://doi.org/10.1061/(ASCE)ST.1943-541X.0000648)


- Fujita K, Takewaki I (2010) Critical correlation of bi-directional horizontal ground motions. *Eng Struct* 32(1):261–272. <https://doi.org/10.1016/j.engstruct.2009.09.013>
- Gao X-A, Zhou X-Y, Wang L (2004) Multi-component seismic analysis for irregular structures. Paper presented at the 13th World Conference on Earthquake Engineering Vancouver, BC
- Gwalani P, Singh Y, Varum H (2021) Effect of Proportioning of Lateral Stiffness in Orthogonal Directions on Seismic Performance of RC Buildings. *J Earthqu Eng* 26(14):7568–7586. <https://doi.org/10.1080/13632469.2021.1964649>
- Ghamry E, Mohamed EK, Sekertekin A, Fathy A (2023) Integration of multiple earthquakes precursors before large earthquakes: a case study of 25 April 2015 in Nepal. *J Atmos Solar Terr Phys* 242:105982. <https://doi.org/10.1016/j.jastp.2022.105982>
- González P (1992) Considering earthquake direction on seismic analysis. Paper presented at the Proceedings of the tenth world conference on earthquake engineering
- Guo Y, Li H, Liang P, Xiong R, Hu C, Xu Y (2024) Preliminary report of coseismic surface rupture (part) of Türkiye's MW78 earthquakes by remote sensing interpretation. *Earthq Res Adv* 4(1):100219. <https://doi.org/10.1016/j.eqrea.2023.100219>
- Haran PD, Davis R, Sarkar P (2015) Reliability evaluation of RC frame by two major fragility analysis methods
- Ibrahim YE, El-Shami MM (2011) Seismic fragility curves for mid-rise reinforced concrete frames in Kingdom of Saudi Arabia. *IES J Part A Civ Struct Eng* 4(4):213–223. <https://doi.org/10.1080/19373260.2011.609325>
- Ibrahim A, Makhloof D, Ren X (2024) Seismic performance and collapse analysis of RC framed-wall structure excited with Turkey/Syria destructive earthquake. Paper presented at the Structures. <https://doi.org/10.1016/j.istruc.2023.105774>
- Irsyam M, Cummins PR, Asurifak M, Faizal L, Natawidjaja DH, Widiyantoro S, Hidayati S (2020) Development of the 2017 national seismic hazard maps of Indonesia. *Earthqu Spectra* 36(1_suppl):112–136. <https://doi.org/10.1177/875529302095120>
- Kanya S, Rao C (2015) Effect of earthquake incidence angle on seismic performance of RC buildings. *Int J Res Eng Technol* 4(13):156–161
- Kassem MM, Nazri FM, Farsangi EN, Ozturk B (2022a) Improved vulnerability index methodology to quantify seismic risk and loss assessment in reinforced concrete buildings. *J Earthq Eng* 26(12):6172–6207. <https://doi.org/10.1080/13632469.2021.1911888>
- Kassem MM, Nazri FM, Farsangi EN, Ozturk B (2022b) Development of a uniform seismic vulnerability index framework for reinforced concrete building typology. *J Build Eng* 47:103838. <https://doi.org/10.1016/j.jobbe.2021.103838>
- Kassem MM, Nazri FM, El-Maissi AM (2023) The influence of slope angle variation on structures resting on hilly region considering soil-structure interaction under earthquake loadings using capacity curves and probabilistic approach. *J Earthq Eng*. <https://doi.org/10.1080/13632469.2023.2256894>
- Kırçıl MS, Polat Z (2006) Fragility analysis of mid-rise R/C frame buildings. *Eng Struct* 28(9):1335–1345. <https://doi.org/10.1016/j.engstruct.2006.01.004>
- Kostinakis KG, Athanatopoulou AM (2015c) Evaluation of scalar structure-specific ground motion intensity measures for seismic response prediction of earthquake resistant 3D buildings. *Earthq Struct* 9(5):1091–1114. <https://doi.org/10.12989/eas.2015.9.5.1091>
- Kostinakis K, Athanatopoulou A, Avramidis I (2013) Evaluation of inelastic response of 3D single-story R/C frames under bi-directional excitation using different orientation schemes. *Bull Earthq Eng* 11:637–661. <https://doi.org/10.1007/s10518-012-9392-5>
- Kumar NK, Gajjar RK (2013) Non-linear response of two-way asymmetric multistorey building under biaxial excitation. *Int J Eng Tech* 5(2):1162–1168
- Kumitani S, Takada T (2009) Probabilistic assessment of buildings damage considering aftershocks of earthquakes. *J Struct Construct Eng* 74(74):459–465. <https://doi.org/10.3130/aijs.74.459>
- Lagaros ND (2010) The impact of the earthquake incident angle on the seismic loss estimation. *Eng Struct* 32(6):1577–1589. <https://doi.org/10.1016/j.engstruct.2010.02.006>
- Lucchini A, Monti G, Kunnath S (2011) Nonlinear response of two-way asymmetric single-story building under biaxial excitation. *J Struct Eng* 137(1):34–40. [https://doi.org/10.1061/\(ASCE\)ST.1943-541X.0000266](https://doi.org/10.1061/(ASCE)ST.1943-541X.0000266)
- MacRae GA, Mattheis J (2000) Three-dimensional steel building response to near-fault motions. *J Struct Eng* 126(1):117–126. [https://doi.org/10.1061/\(ASCE\)0733-9445\(2000\)126:1\(117\)](https://doi.org/10.1061/(ASCE)0733-9445(2000)126:1(117))
- Magliulo G, Maddaloni G, Petrone C (2014) Influence of earthquake direction on the seismic response of irregular plan RC frame buildings. *Earthq Eng Eng Vib* 13:243–256. <https://doi.org/10.1007/s11803-014-0227-z>

- Menun C, Der Kiureghian A (1998) A replacement for the 30%, 40%, and SRSS rules for multicomponent seismic analysis. *Earthq Spectra* 14(1):153–163. <https://doi.org/10.1193/1.1585993>
- Modica A, Stafford PJ (2014) Vector fragility surfaces for reinforced concrete frames in Europe. *Bull Earthq Eng* 12:1725–1753. <https://doi.org/10.1007/s10518-013-9571-z>
- Muntasir Billah A, Shahria Alam M (2015) Seismic fragility assessment of highway bridges: a state-of-the-art review. *Struct Infrastruct Eng* 11(6):804–832. <https://doi.org/10.1080/15732479.2014.912243>
- Newton B (2014) Understanding directionality concepts in seismic analysis. *Memo to Designers*, 20–17.
- Nguyen VT, Kim D (2013a) Influence of incident angles of earthquakes on inelastic responses of asymmetric-plan structures. *Struct Eng Mech Int J* 45(3):373–389. <https://doi.org/10.12989/sem.2013.45.3.373>
- Ni Y, Chen J, Teng H, Jiang H (2015) Influence of earthquake input angle on seismic response of curved girder bridge. *J Traffic Transp Eng (Engl Ed)* 2(4):233–241. <https://doi.org/10.1016/j.jtte.2015.05.003>
- Ozturk B (2017) Seismic behavior of two monumental buildings in historical Cappadocia region of Turkey. *Bull Earthq Eng* 15:3103–3123. <https://doi.org/10.1007/s10518-016-0082-6>
- PEER. (2016). "Pacific Earthquake Engineering Research Centre" <http://peer.berkeley.edu/smcat/data>
- Penzien J, Watabe M (1974) Characteristics of 3-dimensional earthquake ground motions. *Earthq Eng Struct Dyn* 3(4):365–373. <https://doi.org/10.1002/eqe.4290030407>
- Quadri SA, Madhuri M (2014) Investigation of the critical direction of seismic force for the analysis of rc frames. *Int J Civ Eng Technol* 5(6):10–15
- Ramos-Sepúlveda ME, Cabas A (2021) Site effects on ground motion directionality: lessons from case studies in Japan. *Soil Dyn Earthq Eng* 147:106755. <https://doi.org/10.1016/j.soildyn.2021.106755>
- Reyes JC, Kalkan E (2012) Should ground-motion records be rotated to fault-normal/parallel or maximum direction for response history analysis of buildings. *US Geol Surv Open-File Rep* 1261(2012):89
- Reyes JC, Kalkan E (2015) Significance of rotating ground motions on behavior of symmetric-and asymmetric-plan structures: Part I. *Single-Story Struct Earthq Spectra* 31(3):1591–1612. <https://doi.org/10.1193/072012eqs241m>
- Rigato AB, Medina RA (2007) Influence of angle of incidence on seismic demands for inelastic single-storey structures subjected to bi-directional ground motions. *Eng Struct* 29(10):2593–2601. <https://doi.org/10.1016/j.engstruct.2007.01.008>
- Sevim B (2013) Assessment of 3D earthquake response of the Arhavi Highway Tunnel considering soil-structure interaction. *Comput Concr Int J* 11(1):51–61
- Shinozuka M, Feng MQ, Kim H-K, Kim S-H (2000) Nonlinear static procedure for fragility curve development. *J Eng Mech* 126(12):1287–1295. [https://doi.org/10.1061/\(ASCE\)0733-9399\(2000\)126:12\(1287\)](https://doi.org/10.1061/(ASCE)0733-9399(2000)126:12(1287))
- Silva, V., Crowley, H., Varum, H., Pinho, R., & Sousa, L. (2014). Development of a Fragility Model for Moment-frame RC buildings in Portugal Vulnerability, Uncertainty, and Risk: Quantification, Mitigation, and Management (pp. 525–534). <https://doi.org/10.1061/9780784413609.054>
- Smeby W, Der Kiureghian A (1985) Modal combination rules for multicomponent earthquake excitation. *Earthquake Eng Struct Dynam* 13(1):1–12. <https://doi.org/10.1002/eqe.4290130103>
- SNI1726:19. (2019). Indonesia Seismic Resistance Design Guideline for Buildings and Other Structures.
- Tanjung J, Alfajri A (2019) Effect of brick masonry infills to seismic capacity of Indonesia multi-story RC building. *GEOMATE J* 16(57):42–48
- TERDC, T. E. R. D. C. (2007). Specifications for Structures to be Built in Disaster Areas. Ministry of Public Works and Settlement. General Directorate of Disaster Affairs. Earthquake Research Department. Ankara. Turkey. <https://www.deprem.gov.tr>
- Torbol M, Shinozuka M (2012) Effect of the angle of seismic incidence on the fragility curves of bridges. *Earthquake Eng Struct Dyn* 41(14):2111–2124. <https://doi.org/10.1002/eqe.2197>
- Tun M, Htun ZM (2014) Comparison of the effect of irregular high-rise steel building based on different seismic excitation angles. *Int J Sci Eng Technol Res* 3(10):2252–2256
- Wilson EL, Button MR (1982) Three-dimensional dynamic analysis for multi-component earthquake spectra. *Earthq Eng Struct Dynam* 10(3):471–476. <https://doi.org/10.1002/eqe.4290100309>

Publisher's Note Springer Nature remains neutral with regard to jurisdictional claims in published maps and institutional affiliations.

Springer Nature or its licensor (e.g. a society or other partner) holds exclusive rights to this article under a publishing agreement with the author(s) or other rightsholder(s); author self-archiving of the accepted manuscript version of this article is solely governed by the terms of such publishing agreement and applicable law.

Authors and Affiliations

Moustafa Moufid Kassem¹ · Fadzli Mohamed Nazri²  · Zaid A. Al-Sadoon³ · Salmia Beddu¹

✉ Fadzli Mohamed Nazri
cefmn@usm.my

¹ Institute of Energy Infrastructure, Universiti Tenaga Nasional, Jalan Ikram-Uniten, 43000 Kajang, Selangor Darul Ehsan, Malaysia

² School of Civil Engineering, Universiti Sains Malaysia, Engineering Campus, 14300 Nibong Tebal, Penang, Malaysia

³ Department of Civil and Environmental Engineering, University of Sharjah, Sharjah, United Arab Emirates